Geological Survey of Norway
N-7441 Trondheim, Norway
Tel.: 47 73 90 40 00
Telefax 47 73 92 16 20

REPORT

Report no. (NGU): 2004.036
Report no. (SINTEF): 54.5272.00/01/04
ISSN 0800-3416
Grading: Open

Title:
Storage potential for CO_2 in the Beitstadfjord Basin, Mid-Norway

Authors:
Szczepan Polak, Erik Lundin, Reidulv Bøe, Erik Lindeberg, Oddleiv Olesen, & Peter Zweigel

Client:
CO2STORE project group

County:
Norway

Commune:
Inderøy, Mosvik, Verran, Steinkjer

Map-sheet name (M=1:250.000)
Trondheim

Map-sheet no. and -name (M=1:50.000)
1622 II (Verran), 1722 I (Stiklestad), 1723 III (Steinkjer)

Deposit name and grid-reference:

Number of pages: 51 Price (NOK): 320,-
Map enclosures:

Fieldwork carried out:

Date of report:
30.08.2004

Project no.:
299900 (NGU)
54.5272.00 (SINTEF)

Person responsible:
Terje Thorsnes

Summary:

The sedimentary sequence in the subsurface of the Beitstadfjord (Mid-Norway) has been assessed with regard to its suitability for long-term storage of CO_2. This study is part of the EU-funded CO2STORE project and was stimulated by the geographical proximity of the Beitstadfjord Basin to a planned power plant in Skogn where CO_2 may be captured from the flue gas stream.

The sedimentary content of the basin has been interpreted based on seismic data, blocks found at the shore of the fjord, and by analogy to the geology in offshore hydrocarbon fields. The sediments are probably of Jurassic age. Key seismic horizons, including the base of the Quaternary and the top of the basement have been mapped on seismic and depth-converted. Since the basin is nowhere exposed and has not been drilled, the properties of the sedimentary formations are not known. In analogy to the sedimentary succession offshore, two formations with properties suitable for CO_2 injection have been postulated: the 'Ile Formation' and the 'Garn Formation'. These formations form no traps but dip towards northwest.

A digital subsurface geology model has been generated based on the mapped horizons. Petrophysical properties of the potential reservoir formations are only tentatively known from offshore analogs. Therefore several cases with variable reservoir properties and variable properties of the seal (the Quaternary) have been simulated. The key simulations assume co-injection into both postulated reservoir formations. The simulation results show that if the Quaternary has a low permeability, it can retain CO_2 initially. However the pore pressure in the reservoir will very fast increase to a level at which the seal will undergo hydraulic fracturing, that is, it will acquire a high permeability at which CO_2 will leak fast.

Alternatively, if the Quaternary has a relatively high permeability to avoid pressure build-up to critical levels, leakage rates for the CO_2 will be very high and the majority of the injected CO_2 will have leaked already 50 years after injection start.

The conclusion of this assessment is thus that the Beitstadfjord Basin is not suitable for long-term CO_2 storage. The major problem with the Beitstadfjord Basin appears to be a too small available pore volume for storage of economically viable CO_2 quantities.

Keywords: Aquifer	CO_2	Carbondioxide storage
Reservoir simulation	Numerical modelling	Beitstadfjorden
Leakage rate	Storage capacity	Jurassic

CONTENTS

FIGURES

Figure 18 Simulated cumulative volume of CO_2 leaked from the reservoirs for the case of co-injection into the ‘Ile’ and ‘Garn’ formations, for four different low seal permeabilities (kQ). All cases with kQ lower than 0.1 mD yielded no significant leakage during the simulated 50 years.

Figure 19 Simulated average reservoir pressure for the case of co-injection into the ‘Ile’ and ‘Garn’ formations, for two different high seal permeabilities (kQ). Upper: in the ‘Ile Formation’; lower: in the ‘Garn Formation’.

Figure 20 Simulated cumulative volume of CO_2 leaked from the reservoirs for the case of co-injection into the ‘Ile’ and ‘Garn’ formations, for two different high seal permeabilities (kQ). The cumulative injected volume of CO_2 is also shown.

Figure 21 Simulated average reservoir pressure for the case of co-injection into the ‘Ile’ and ‘Garn’ formations, for three combinations of high seal permeabilities (kQ) with reservoir permeability and net reservoir porosity. Upper: in the ‘Ile Formation’; lower: in the ‘Garn Formation’.

Figure 22 Simulated cumulative volume of CO_2 leaked from the reservoirs for the case of co-injection into the ‘Ile’ and ‘Garn’ formations, for three combinations of high seal permeabilities (kQ) with reservoir permeability and net reservoir porosity. The cumulative injected volume of CO_2 is also shown. Upper: first 50 years from injection start; lower: first 500 years (two cases only) .

Figure 23 Simulated average reservoir pressure for the case of injection into the ‘Ile’ Formation only, for three different high seal permeabilities (kQ).

Figure 24 Simulated cumulative volume of CO_2 leaked from the reservoir for the case of injection into the ‘Ile’ Formation only, for three high seal permeabilities (kQ).The cumulative injected volume of CO_2 is also shown.

Figure 25 Simulated average reservoir pressure for the case of injection into the ‘Ile’ Formation only with a hole in the seal (Quaternary), for five different seal permeabilities (kQ, relative permeability for water and gas).

Figure 26 Simulated cumulative volume of CO_2 leaked from the reservoir for the case of injection into the ‘Ile’ Formation only with a hole, for five different seal permeabilities (kQ, relative permeability for water and gas).The cumulative injected volume of CO_2 is also shown.

Figure 27 Simulated average reservoir pressure for the case of injection into the ‘Garn’ Formation only, for two different high seal permeabilities (kQ).

Figure 28 Simulated cumulative volume of CO_2 leaked from the reservoir for the case of injection into the ‘Garn’ Formation only, for two high seal permeabilities (kQ).The cumulative injected volume of CO_2 is also shown.

Figure 29 CO_2 viscosity vs. pressure at reservoir temperature of 31^oC

Figure 30 Density of reservoir water at different CO_2 saturation vs. pressure at reservoir temperature of 31^oC

Figure 31 Viscosity of reservoir water at different CO_2 saturation vs. pressure at reservoir temperature of 31^oC

Figure 32 Results of simulated cases of injection into the ‘Ile Formation’ only and for four different low seal permeabilities (kQ). Upper: simulated average reservoir pressure; lower: simulated cumulative volume of CO_2 leaked from the reservoir.

Figure 33 Results of simulated cases of injection into the ‘Ile Formation’ only and for four different low seal permeabilities (kQ). Upper: simulated average reservoir pressure; lower: simulated cumulative volume of CO_2 leaked from the reservoir (note the scale of the vertical axis).

TABLES

1. EXECUTIVE SUMMARY

Plans for a combined heat and power plant (CHP) in Skogn in the inner part of the Trondheimsfjord (Mid-Norway) include options to capture CO_2 from the flue gas stream. In order to reduce anthropogenic greenhouse gas emissions, several potential sites for underground storage of CO_2 are investigated as part of the EU- and industry-funded project CO_2STORE. One of the potential storage sites in Mid-Norway is the Beitstadfjord Basin, which is a sedimentary basin immediately adjacent to the site of the planned CHP. This report documents the results of an assessment of the subsurface sedimentary succession of the Beitstadfjord with regard to its suitability for long-term storage of CO_2.

The objective of the assessment is to predict if CO_2 injected at the typical emission rate from a CHP of approximately 2 000 000 tonnes per year would stay in the subsurface and would leak - if at all – at a rate acceptable to reach long-term goals for maximum atmospheric CO_2 concentrations. Alternatively, injection may take place at a rate of only 100 000 tonnes per year, corresponding to the captured mass in a test facility capturing only 5 % of the total emissions from the plant. The suitability of the site for injection at this rate should also be assessed.

The geometry and sedimentary content of the basin have been interpreted from seismic data. The basin forms a half-graben with a major normal fault at its northwestern margin. Four main sedimentary units have been distinguished, three of which (named seismic units A, B, and C) dip towards the northwest (Figure 1). The Quaternary, as the fourth sedimentary unit, overlies the other formations discordantly. It has a thickness of up to approximately 200 m, but is mostly much thinner and is possibly locally absent forming ‘holes’.

The basin has not been drilled and information about the age and lithology of the three pre-Quaternary units has therefore been derived from blocks found at the shores of the Beitstadfjord. These blocks indicate a Jurassic age. The three units have tentatively been correlated to formations known from numerous wells in the offshore hydrocarbon province of the Halten Terrace, among them two formations with possibly favourable reservoir properties: the ‘Ile’ and ‘Garn’ formations. According to the seismic data, these formations do not form traps in the Beitstadfjord Basin.

A digital subsurface geology model has been generated based on the mapped horizons. Since the petrophysical properties of the potential reservoir formations are not known due to the lack of wellbore data, they had to be estimated based on the offshore geological analogs. The implicit uncertainty was addressed by simulation of a range of cases with varying reservoir properties, and particularly with varying fluid-flow relevant properties of the seal (the Quaternary).

At the probable pressure and temperature conditions in the Beitstadfjord Basin, CO_2 will have a relatively high density of approximately 800 kg/m^3 below a depth of about 500 m bsl. This is lower than the density of the formation water. The main process expected to occur in case of CO_2-injection in the Beitstadfjord Basin is buoyancy-driven upward migration until the CO_2 reaches an impermeable formation. It will then migrate upwards along the top of the reservoir formation until it either reaches a final seal or it escapes into the sea water in the Beitstadfjord. Some CO_2 will be dissolved into formation water in the reservoir unit, but this process is slow, operating over a time scale of 1000s of years.

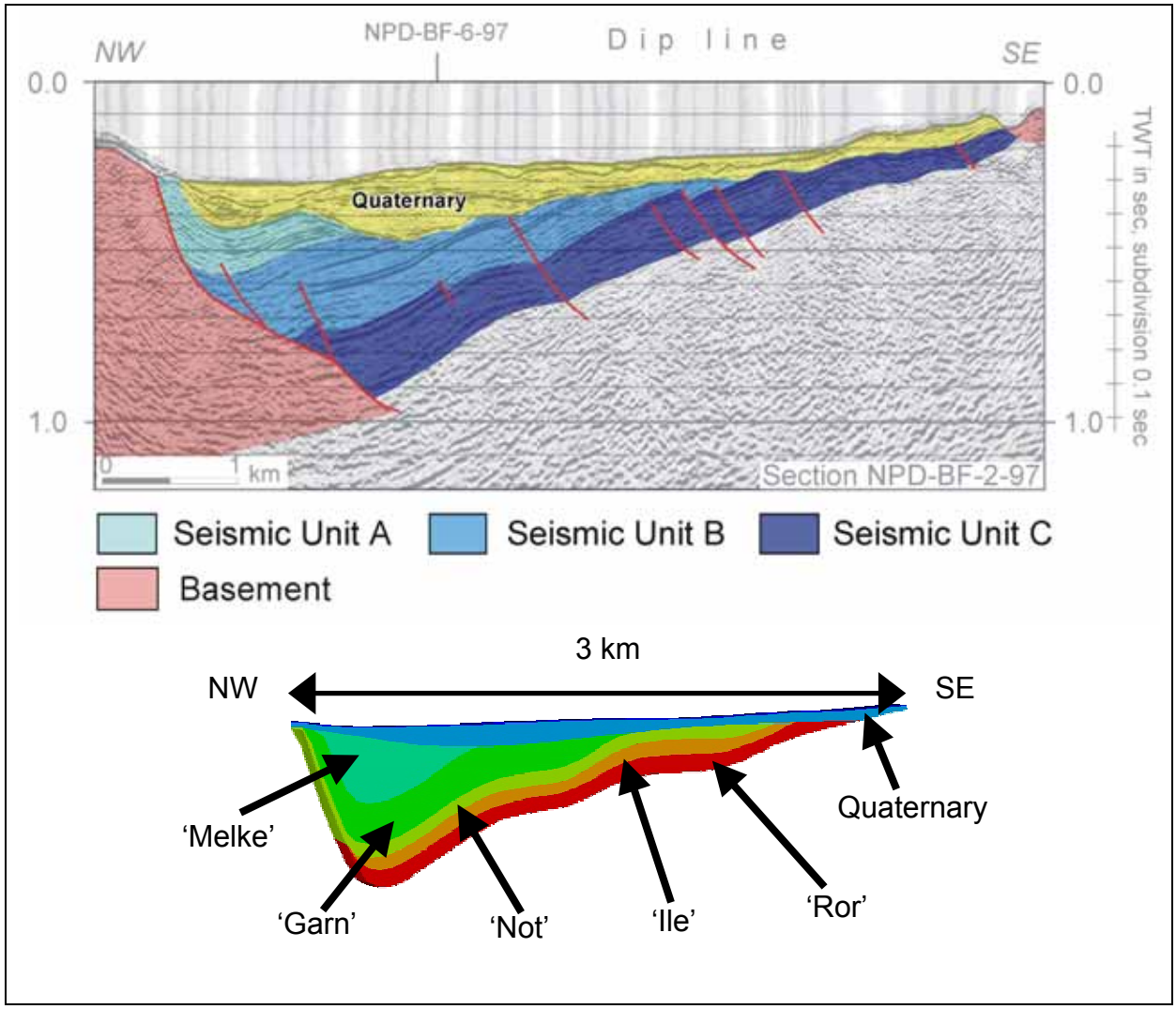

Figure 1 *Cross section through the Beitstadfjord Basin. Upper: Seismic section with main seismic units. Lower: representation in the geological model and terminology in analogy to the offshore area.*

If formation water and CO_2 can leave the storage reservoir only at a very low rate, pore pressure in the reservoir will increase. This pore pressure increase may induce hydraulic fracturing of the seal, generating highly efficient pathways for pressure release and migration of CO_2 from the reservoir unit into the sea water. It is estimated that a pore pressure increase in the reservoir of more than 3.6 bars may cause hydraulic fracturing of the seal.

Reservoir simulations were carried out to test if CO_2 injected at a rate of 2 million tonnes per year would leak from the reservoir or if it would induce pore pressures causing hydraulic fracturing of the seal. The key simulations assume co-injection into the 'Ile' and 'Garn' formations with injection rates per formation being proportional to their calculated pore volume.

The simulation results show that if the Quaternary seal has a low permeability of approximately 0.1 milliDarcy (mD) or less, it can retain CO_2 initially. However the pore pressure in the reservoir will very fast increase to a level at which the seal will undergo

hydraulic fracturing, that is, it will acquire a high permeability at which CO_2 will leak rapidly. Pressure build-up will occur also at higher permeabilities up to approximately 1000 mD.

Alternatively, if the Quaternary has high permeability (more than 1000 mD), the pressure will not build-up to critical levels, but the leakage rates for the CO_2 will be very high and the majority of the injected CO_2 will have leaked already 50 years after injection start. Leakage may be somewhat slower if the reservoir permeability is lower than in the base case (which is 2000 mD horizontal permeability), but also here the large majority of injected CO_2 will have leaked after 500 years. Simulated cases of injection into only one of the two compartments yield even less favourable results.

Estimates based on the simulation results indicate that pressure build-up in case of a low-permeable seal and leakage rates in case of a high-permeable seal will also be unacceptable if injection would take place at a much lower rate of only 100 000 tonnes/year. This corresponds to approximately 5% of the potential emissions of the planned power plant.

The conclusion of this assessment is thus that the Beitstadfjord Basin is not suitable for long-term CO_2 storage, not even at a modest injection rate. The major problem with the Beitstadfjord Basin as a CO_2 storage site is a too small available pore volume in the potential storage formations.

2. INTRODUCTION

Industrikraft Midt-Norge (IMN) is planning to build a combined heat and power plant (CHP) at Fiborgtangen in Skogn (Figure 2) in the inner part of Trondheimsfjorden. The plant shall utilize natural gas from Haltenbanken, off Mid-Norway. Capture of a large part or at least of a fraction of the produced carbon dioxide (CO_2) from the power plant is being evaluated as an option to reduce greenhouse gas emissions.

Previous work in the EU-funded GESTCO project (Bøe et al. 2002) has identified potential sites for underground long-term storage of CO_2 in the vicinity of the power plant. Among these sites are the Beitstadfjord and Frohavet Basins and the southeastern part of the Trøndelag Platform (Figure 2). CO_2 storage in oil and gas fields on the Halten Terrace will not be possible in the next ten to twenty years (except for enhanced oil recovery) due to probable conflicts with hydrocarbon exploitation.

The Beitstadfjord Basin is situated close to the location of the planned power plant, therefore costs for a CO_2-pipeline from the power plant to the storage site might be low. This site has accordingly been mentioned several times in public discussion. However, its technical suitability for underground CO_2 storage has not yet been assessed.

With this background, it was decided to include the technical asessment of this site in the partly EU-funded project CO2STORE (http://www.co2store.org/), which runs from 2003 to 2005 and which aims to prepare the ground for widespread underground storage of CO_2. One part of the CO2STORE project is the identification and first assessment of potential storage sites in four European countries.

One of the regions to be investigated is Mid-Norway (‘Feasibility Case Study Mid-Norway’, www.ngu.no/CO2STORE), and three geographical areas shall here be studied: the Beitstadfjord Basin, the Frohavet Basin and the Trøndelag Platform, southeast of the hydrocarbon province in Haltenbanken. The Beitstadford Basin has been studied first because its position is closest to the potential CO_2-producer. The Feasibility Case Study Mid-Norway is carried out in cooperation between the Geological Survey of Norway (NGU), SINTEF Petroleum Research, Industrikraft Midt-Norge (IMN) and Statoil.

The objectives of this feasibility case study are to:

- Identify suitable saline aquifers for underground CO_2 storage on the southeastern part of the Trøndelag Platform and in the Beitstadfjord and the Frohavet basins.Determine storage capacity by regional mapping, reservoir parameter quantification, and simulation of migration and underground behaviour of CO_2 in these aquifers.
- Investigate and evaluate stability of CO_2 storage in the study area. The risk for, mechanism behind and effect of potential leakages from the storage formations shall be studied.
- Suggest further investigations of prospective aquifers.

In this report, the results of the mapping, reservoir parameter quantification and migration simulation for the Beitstadfjord Basin are summarized, and the suitability of the Beitstadfjord Basin for underground CO_2 storage is evaluated.

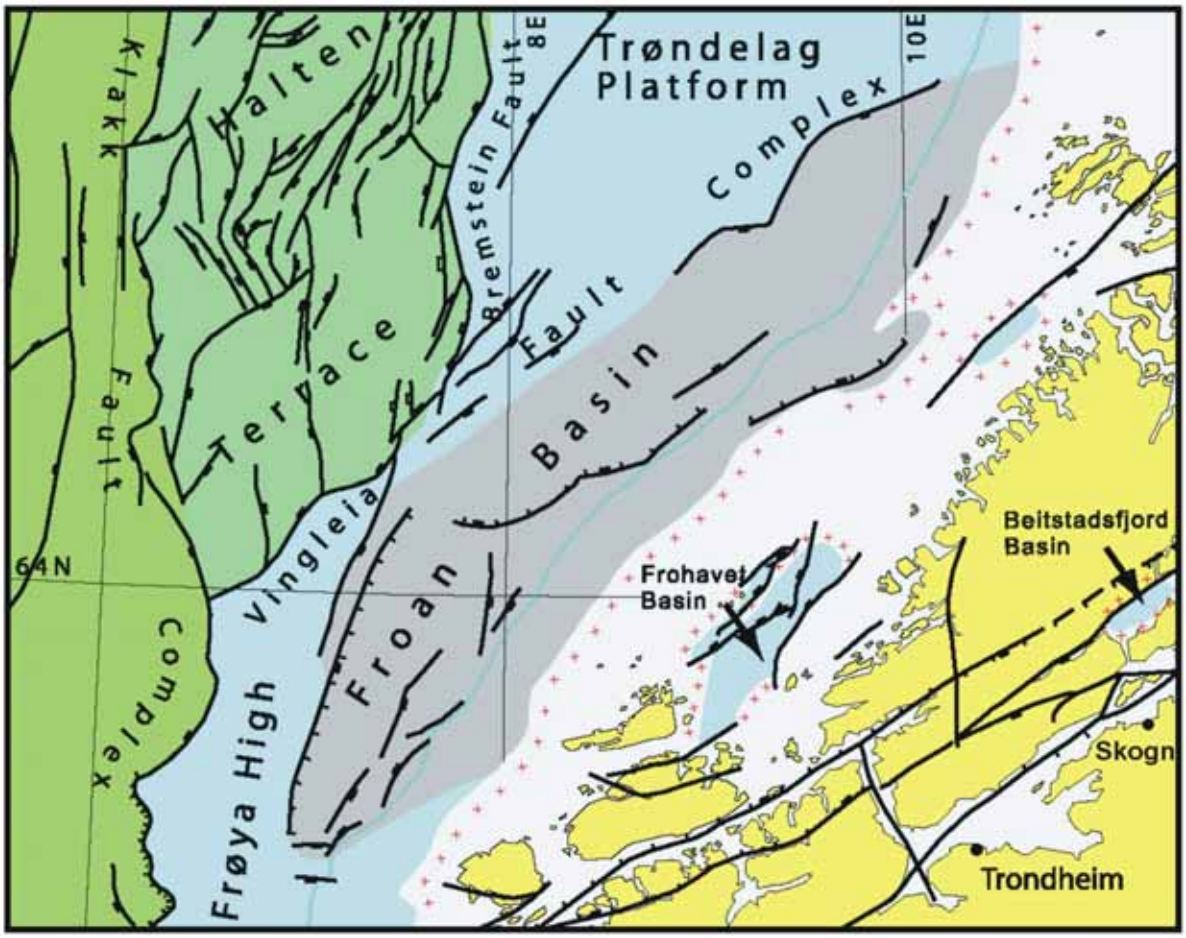

Figure 2 *Geological map of Mid-Norway showing the main structural provinces. The location of Skogn and the Beitstadfjord Basin are shown in the inner part of the Trondheimsfjord. Modified from Blystad et al. (1995).*

3. GEOLOGY OF THE BEITSTADFJORD BASIN

3.1 Seismic database

The Beitstadfjord Basin is sparsely covered by 2D multichannel seismic data. Six seismic profiles, totalling 57 km in length, were acquired as part of the Kyst-97 survey by the Norwegian Petroleum Directorate. In addition, NGU has acquired 290 km single channel seismic profiles in the Beitstadfjord (Figure 3, Bøe & Bjerkli 1989, Sommaruga & Bøe 2002). The Kyst-97 data penetrates the entire sedimentary succession, while the NGU data only image the upper 0.350 s TWT (seconds two-way travel time). In this project, the Kyst-97 profiles were used for mapping. Earlier interpretations (Bøe & Bjerkli 1989, Sommaruga & Bøe 2002) were used in areas not covered by the Kyst-97 data.

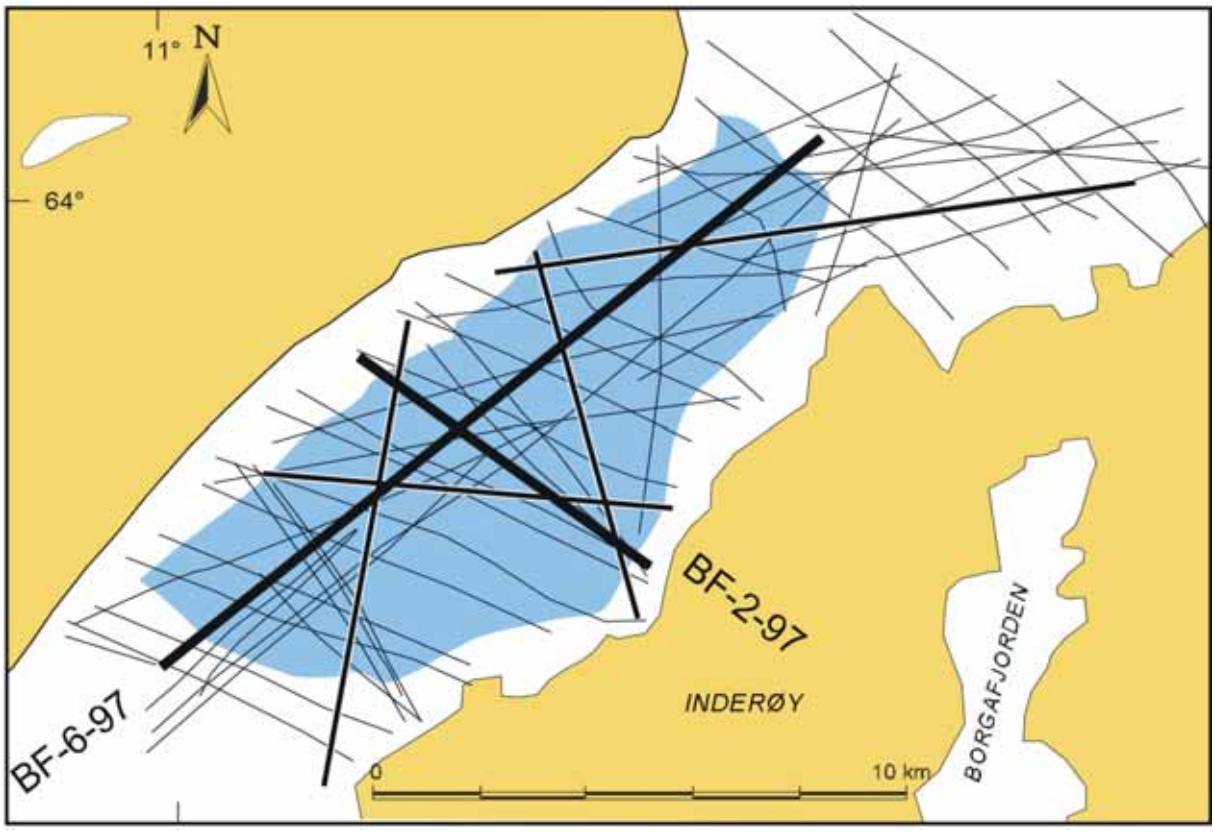

Figure 3 *Seismic grid in the Beitstadfjord. The Jurassic Beitstadfjord Basin is shown in blue. Modified from Sommaruga & Bøe (2002).*

3.2 Bathymetry

The Beitstadfjord reaches a maximum water depth in excess of 200 m in its southwestern part (Figure 4). There is a gradual decrease in water depth towards the east and northeast. Above the geographical area of the Jurassic Beitstadfjord Basin (see below) water depths are everywhere more than 100 m, except for a small area in the east, where it is close to 50 m.

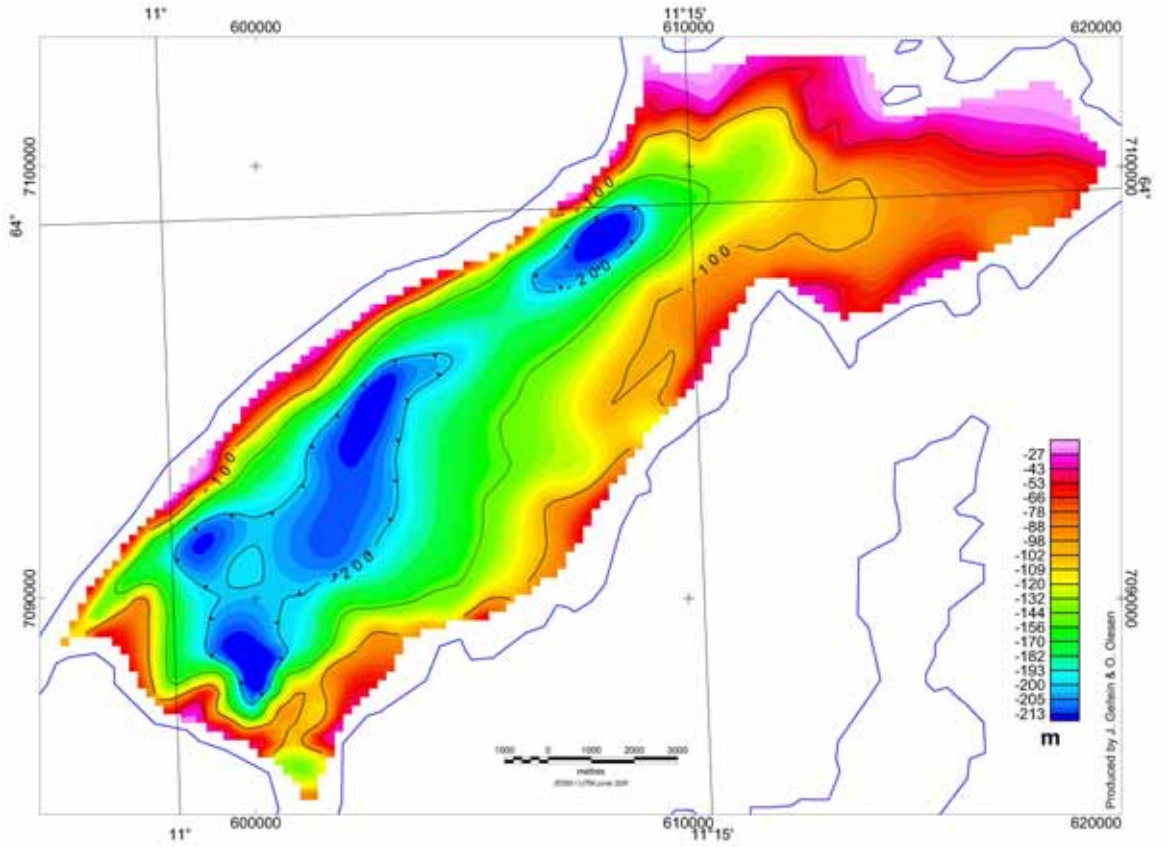

Figure 4 *Bathymetry of the Beitstadfjord. The digital map is based on the bathymetry map in Bøe & Bjerkli (1989).*

3.3 Quaternary deposits

In the Beitstadfjord, there is a succession of Quaternary deposits varying in thickness from a few metres to approximately 200 m (Figure 5, Figure 6) (Bøe & Bjerkli 1989). The thickness of the succession on top of the Jurassic Beitstadfjord Basin (see below) is only rarely less than 30 m. The succession is dominated by till, but also marine and glaciomarine, fine-grained sediments occur. Erratic fragments of Middle Jurassic age are found in till and marginal marine deposits along the western shores of the Beitstadfjord. These were eroded from the Jurassic Beitstadfjord Basin and deposited by ice streams moving in westerly directions during the final stages of the last glaciation.

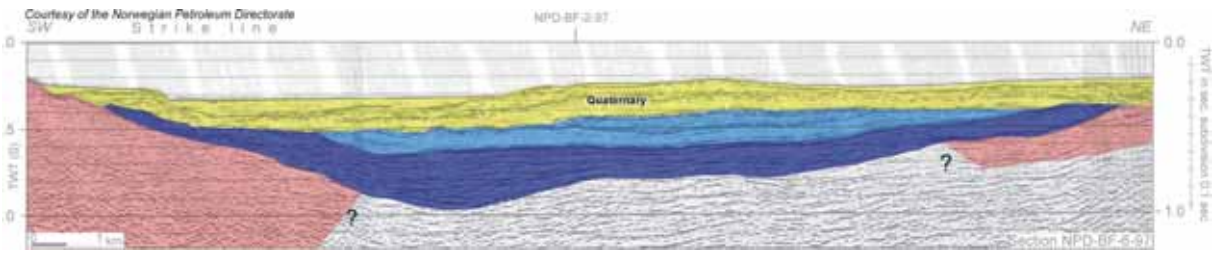

Figure 5 *Interpreted seismic line across the Beitstadfjord. See Figure 3 for location of the seismic profile and Figure 8 for colour legend. Modified from Sommaruga & Bøe (2002).*

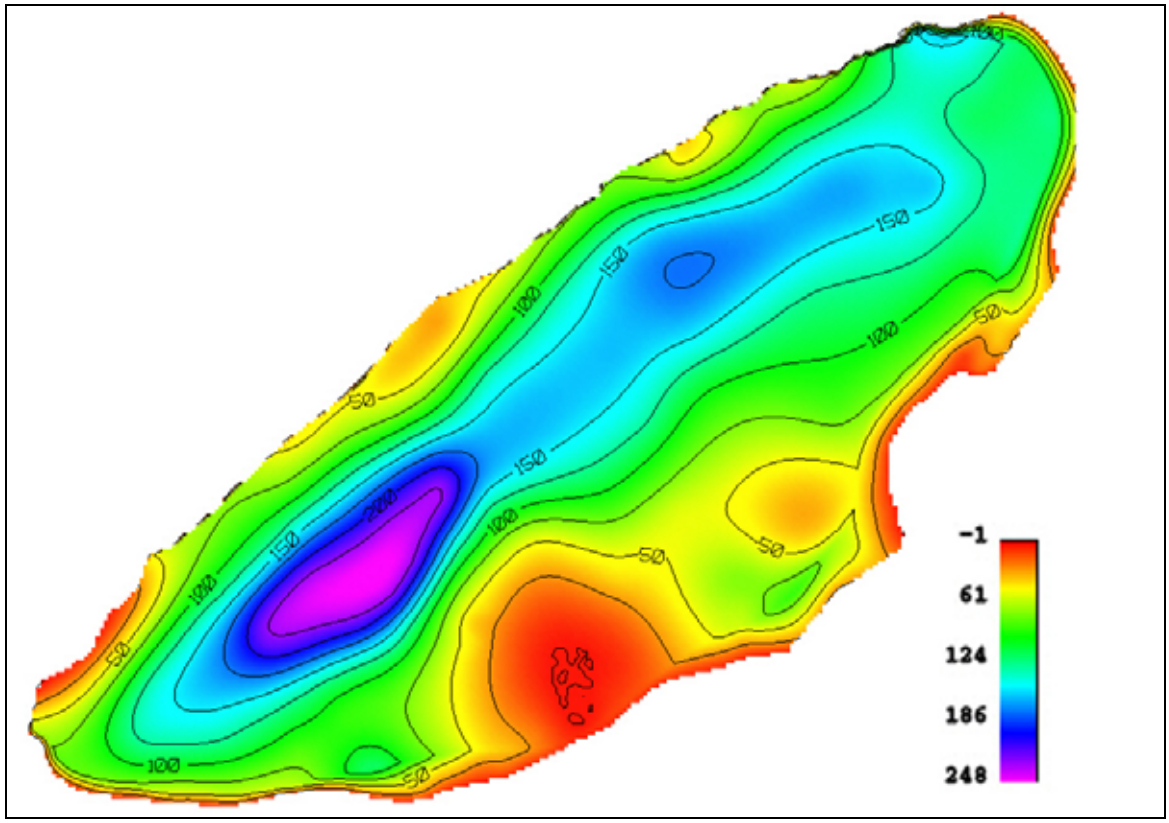

Figure 6 *Thickness map of the Quaternary. The area within the 0 m isoline (center of the red area) has a very thin or absent Quaternary cover; however there is some uncertainty due to the interpolation procedure between seismic lines. All values and isolines in meters.*

3.4 Geometry, sedimentary content, and burial/uplift history

The Beitstadfjord Basin, which contains a sedimentary rock succession of Middle Jurassic age, is an approximately 14 km long by 6 km wide, NE-trending half graben located at the northeastern extremity of the Trondheimfjord (Figure 7, Oftedahl 1972, Bøe & Bjerkli 1989, Sommaruga & Bøe 2002). The basin is surrounded by Precambrian migmatitic rocks to the north and Lower Palaeozoic metasediments to the south (Figure 7, Sommaruga & Bøe 2002). The half graben dips to the NW, against its bounding normal fault (Figure 7 and Figure 8) while to the southwest, southeast and northeast the Jurassic rocks lie unconformably on basement (Figure 5, Figure 7, Figure 8). The basin occurs along the Møre-Trøndlag Fault Complex (MTFC), which is a major Caledonian strike slip structure that has experienced several phases of movement between Devonian and Tertiary time (Gabrielsen et al. 1999).

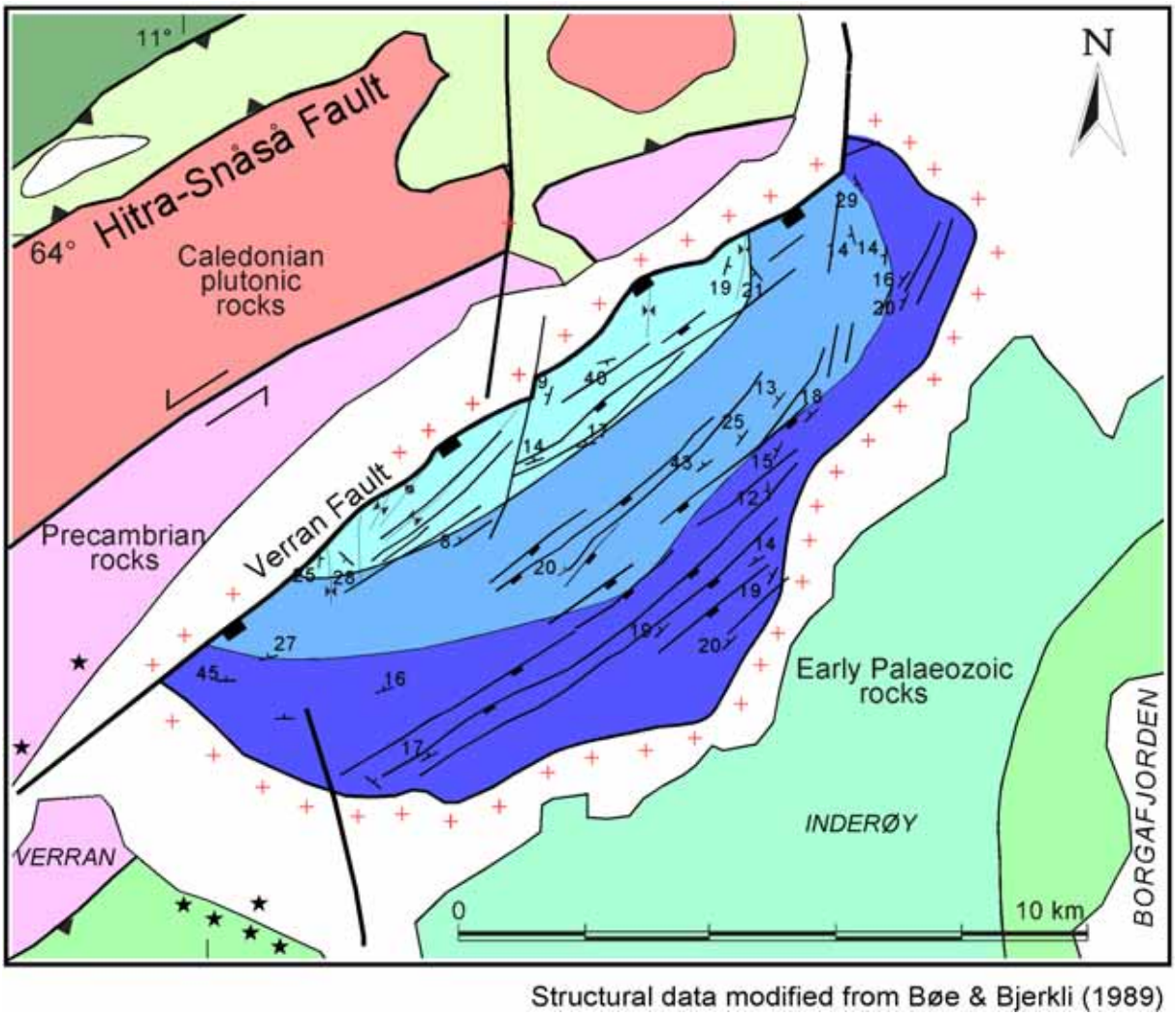

Figure 7 *Geological map of the Beitstadfjord Basin. See Figure 8 for colour legend. Modified from Sommaruga & Bøe (2002). Asterixes show the location of Middle Jurassic fragments found along the shores of the Beitstadfjord.*

Based on seismic character, the dipping succession has been divided into units A-C (Sommaruga & Bøe 2002) (Figure 5, Figure 7, Figure 8). These workers postulated that the three units are correlative with the Middle Jurassic Ile, Garn, and Melke Formations known offshore mid-Norway. However, there is no well control in the Beitstadfjord Basin, and besides seismic character, the age and type of basin fill has only been estimated from loose fragments found on nearby shores (Figure 7). These are made up of Middle Jurassic sideritic ironstone and sandstone, and the petrology/chemical composition and the fossil content suggest deposition in shallow lakes in a warm climate (Oftedahl 1972).

When found on the shore, the sideritic ironstone fragments display a rust-coloured to yellowish-brown crust. On their fresh surfaces, most sideritic blocks are medium grey in colour and fine-grained. Under the microscope, the carbonate phase is always strongly coloured and pigmented, usually in a deep brownish colour, but occasionally in pure grey. Some of the boulders contain unoriented black remnants of plant stems and leaves (Figure 9). A few of the boulders are very rich in organic material, some are clearly layered, and quarts pebbles up to 1 cm occur (Oftedahl 1972). Petrographical and chemical anlysis carried out on

7 sideritic ironstones from the shores of the Beitstadfjord show that they contain up to 50% FeO, 56-83% siderite, 9-24% kaolinite, 1-8% hematite and only a few percent quartz and muscovite (Oftedahl 1972). Many samples reveal sand grains essentially floating in a carbonate matrix, indicating very early cementation, prior to any significant compaction. Sandstones may contain up to 80% quartz; 26% of the samples contain more than 30% quartz.

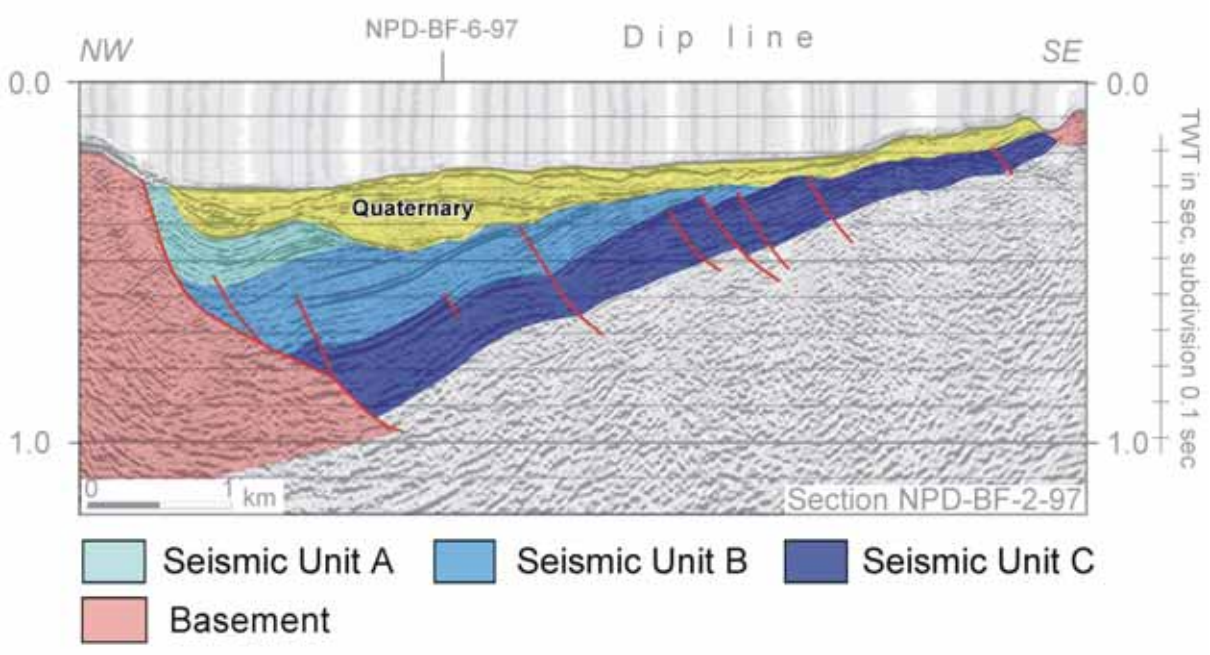

Figure 8 *Interpreted seismic line across the Beitstadfjord. Note that the Jurassic sedimentary succession is downthrown in the northwest along a fault that is a branch of the Verran Fault System. See Figure 3 for location of the seismic profile. Modified from Sommaruga & Bøe (2002).*

The basin is relatively shallow, with a maximum depth of approximately 1.0 s TWT (ca. 1.3 km, see chapter on depth conversion). It is clear that the basin has been uplifted and significantly eroded. Evidence for the uplift are provided by: a) seismic velocities (Oftedahl 1975) that are too high for the current basin depth, b) maturation of coal (Weisz 1992), and c) truncation of the dipping Middle Jurassic beds below the Quaternary unconformity. It is likely that local areas along the MTFC, such as the Beitstadfjord, have experienced vertical motions related to strike-slip motion of the MTFC, in addition to the regional Neogene uplift of the Norwegian mainland (e.g. Riis 1996).

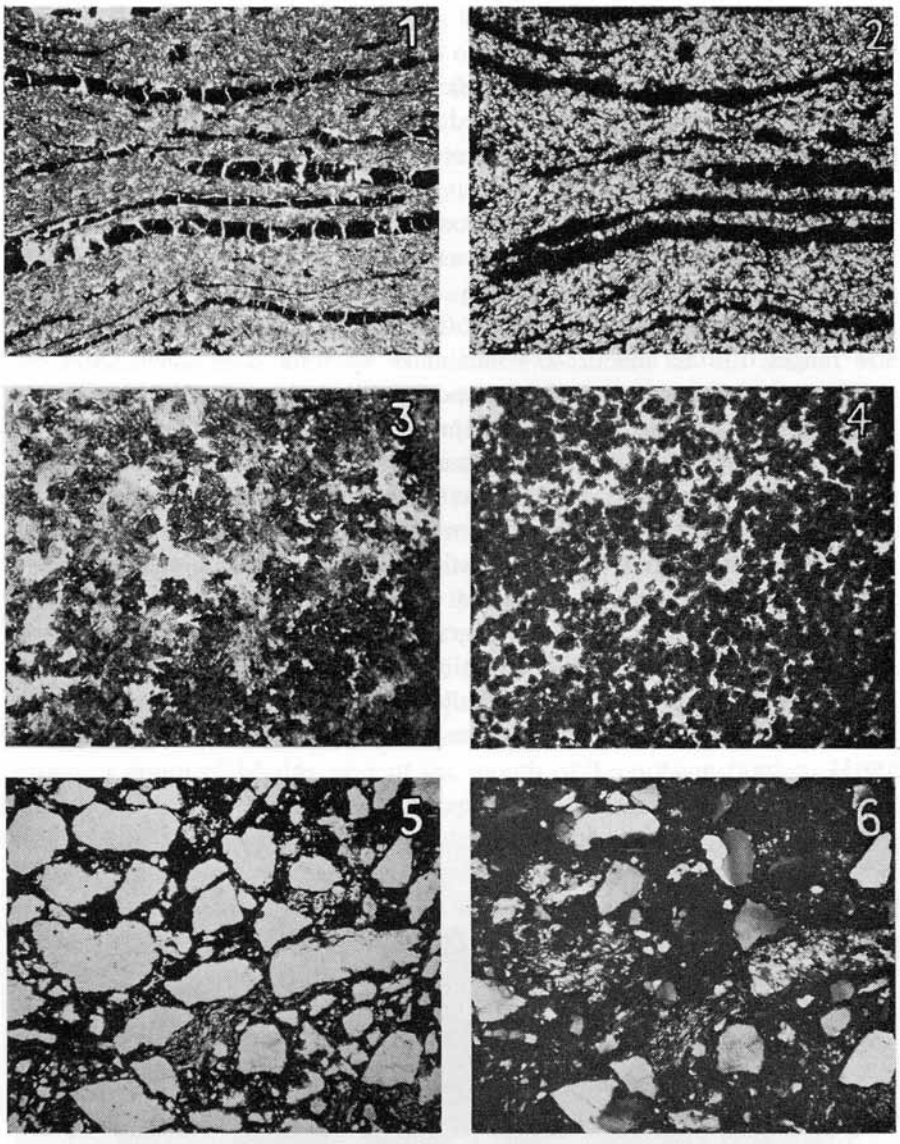

Figure 9 *Photomicrographs of ironstones from the Beitstadfjord. 1-2: Plant leaves with fractures filled with kaolinite in a groundmass of fine-grained siderite. 3-4: Siderite with white areas of kaolinite. 5-6: Poorly sorted sandstone with angular sandstone grains. From Oftedahl (1972).*

An important consequence of uplift and erosion is that the basin is more compacted than it would have been otherwise, and that Cretaceous and younger successions have been removed. In general, porosity and permeability are related to compaction, which in turn is related to the maximum burial depth. The process of compaction is irreversible. Compaction influences seismic velocity, and thus, a relationship exists between seismic velocity and maximum burial depth (Sheriff 1989). Refraction seismic data from the Beitstadsfjord reveal an average velocity of 3.6-3.7 s/km for the Middle Jurassic strata (Oftedal 1975). For a sand-shale sequence such a velocity would correspond to a burial depth of approximately 4 km (Sheriff 1989). If one assumes that the refraction velocity represents a headwave from the top of the truncated Jurassic beds, situated at ca. 350 m depth, this implies an uplift of approximately 3.6 km. The Jurassic thickness is up to approximately 0.5 s TWT, or ca. 900 m, meaning that the maximum burial depth of the deepest part of the basin was approximately 4.5 km. On the other hand, organic matter maturation mesured on Middle Jurassic sandstone fragments found

along the shores of the Beitstadfjord (Oftedahl 1972) suggests a maximum burial depth of 1.8-2.3 km (Weisz 1992). Assuming an average value of 2 km results in a basin depth range of 2-3 km since the loose fragments were plucked by an overriding glacier at the Quaternary unconformity level. Finally, a regional assessment of net Neogene uplift suggests that the Beitstadsfjord area is only uplifted ca. 750 m (Riis 1996). The latter estimate needs not be inconsistent with the previous since more than one post-Jurassic uplift event may have taken place.

3.5 Time-depth conversion of seismic data

Depth converted time structure maps of base Quaternary, top Unit C, and top basement are shown in Figure 10, Figure 11, and Figure 12. The velocity for the Quaternary succession is based on the assumption that the sequence is made up mainly of moraine (Table 1). The value of 2.0 km/s lies within the range of velocities typically found for moraines (Blikra et al. 1991). The velocity of the Jurassic succession is based on refraction velocities from the Beitstadsfjord Basin (Oftedal 1975).

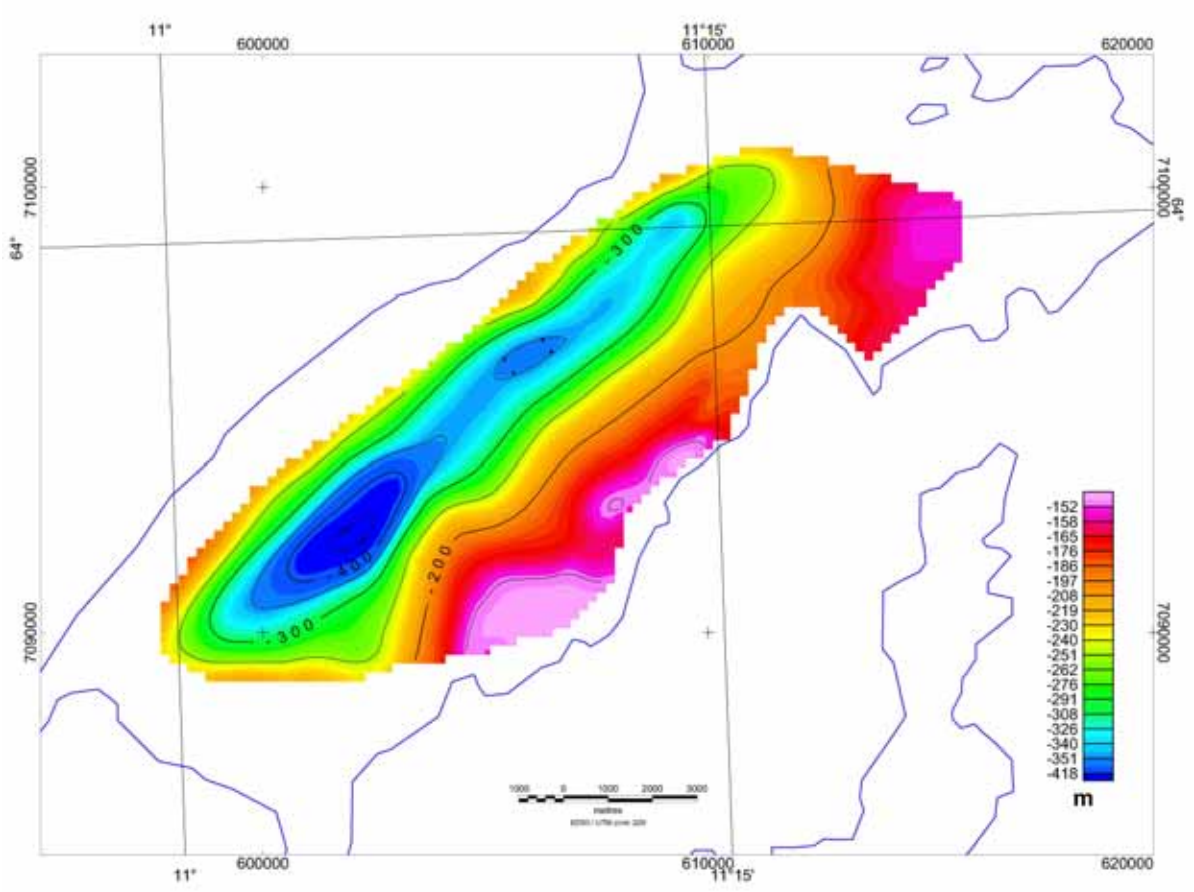

Figure 10 Depth (m) to base Quaternary in the Beitstadfjord.

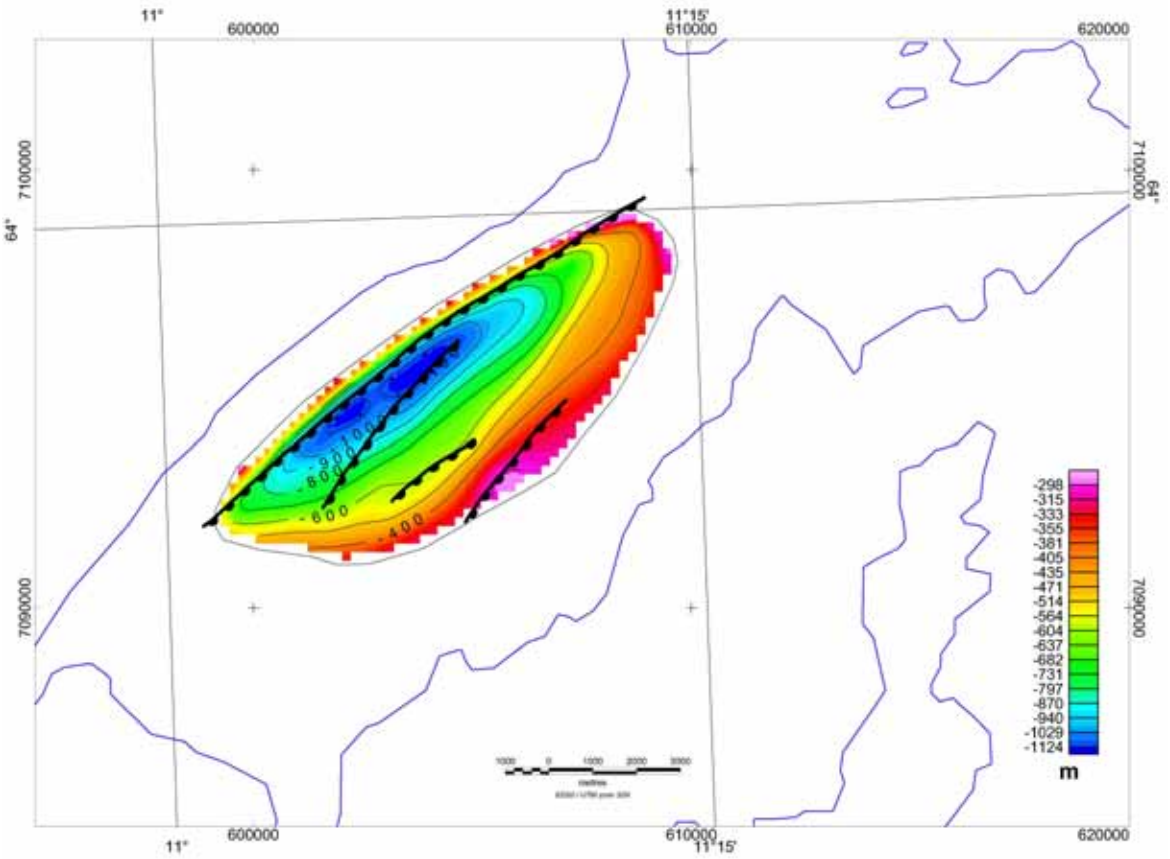

Figure 11 Depth (m) to top Unit C in the Beitstadfjord Basin.

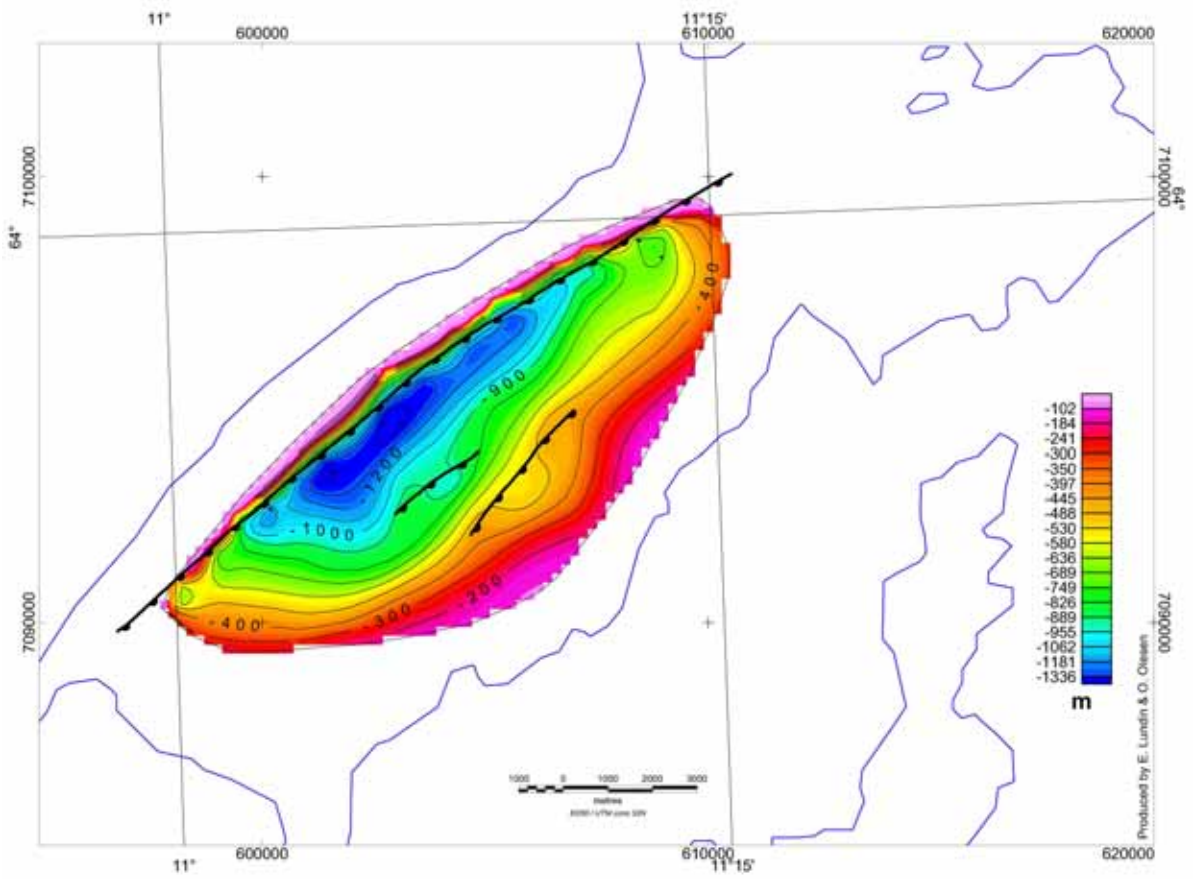

Figure 12 Depth (m) to top basement, below the Beitstadfjord Basin.

Table 1. Velocities used to depth convert time structure maps from the Beitstadfjord.

Interval	Velocity
Sea water	1.48 km/s
Quaternary deposits (mainly moraine)	2.0 km/s
Jurassic sedimentary rocks	3.6 km/s

3.6 Key features of Beitstadfjord Basin geology as input to reservoir simulation

The Beitstadfjord Basin is characterized by a simple geometry, homoclinally dipping to the northwest. Although some minor faults do exist within the basin, these are not considered to be large enough to generate significant independent traps. With the present poor knowledge of the basin stratigraphy, it appears inappropriate to include possible fault barriers in a model. Thus, for the modelling purposes, the basin is treated as a simple NW-dipping homocline. The basin subcrops below the Quaternary cover, which is not considered to be an efficient top seal.

There is currently no basis for subdividing the basin fill into sandstone versus shale sequences. Lacking knowledge of the actual stratigraphy, a hypothetical aquifer has been

placed directly over basement. In doing so, one achieves an optimistic position of an aquifer, since storage of CO_2 should be performed at a depth of at least ca. 800 m. Suggesting a much shallower aquifer would immediately rule out the basin as a possible depository of CO_2, making modelling redundant. The thickness of the aquifer is unknown, and cannot be assessed from the seismic data. For the purposes of modelling a range is given. If the deepest possible aquifer is shown to be unsuitable after the modelling is performed, one can rule out the basin as a potential storage site for CO_2. Should the modelling yield an acceptable result, actual stratigraphy and aquifer properties should be established by stratigraphic drilling.

Of the three different estimates of maximum burial depth (see above), the deepest is regarded unrealistically deep. The velocity-based estimate is twice as deep as the estimate based on organic matter maturation. If the velocity-based depth of burial was used the entire assumed aquifer would be below the typical depth for rapid deterioration of permeability at 3.6 km (Ehrenberg 1990), rendering a tight aquifer. Thus, the deepest scenario is not considered since that would make the modelling redundant. Both the velocity-based and the organic maturation-based estimates of depth of burial are considerably larger than the estimate based on mapping paleic surfaces onshore and comparing with the Mesozoic and Cenozoic subcrop offshore (Riis 1996). However, the discrepancy with the estimated Neogene uplift may relate to older uplift events.

For the purpose of modelling fluid flow in the basin, the deepest estimate would yield very poor aquifer properties. As viewed here, the purpose of the modelling is to provide a first order feasibility test of the assumed aquifer. Thus, neither the deepest nor the shallowest estimates of maximum depth of burial are selected for modelling. Aquifer properties are chosen based on the organic matter estimate. Within the given burial depths between 1.8 and 2.3 km, a value of 2.0 km is for the shallowest part of the basin, while the deepest is ca 3.0 km.

The porosity of the sandstone blocks is generally poor due to significant cementation (Figure 9). On the sideritic ironstones, Oftedahl (1972) measured porosities of 0.6-2.1%. These highly cemented samples are considered unrepresentative of the basin sequence as a whole since they likely are preferentially preserved because of their resistance to erosion; the preserved blocks are thought to represent highly cemented layers. Some samples do show better porosity. Similar samples from Froan have yielded porosities up to 8%, but also these are considered to be unrepresentative; porosities up to 20% should be expected in less cemented layers (Mørk et al. 2003).

The closest shallow IKU stratigraphic wells that have drilled Jurassic sequences are wells 6206/02-U01, 02, 03 and 08, located ca. 260 km to the southwest of the Beitstadsfjord. However, a large number of exploration wells have drilled the Jurassic successions in the Haltenbanken province, ca. 230 km to the northwest.

Density, viscosity, and solubility of CO_2 are sensitive to temperature. A temperature of ca 29 °C at 1200 m below sea floor has been reported from the Malm mines, located immediately north of the Beitstadfjord (Arne Myrvang, pers. comm. 2003).

4. RESERVOIR SIMULATION

4.1 Rationale

The goal of the reservoir simulation study is to find out if the Beitstadfjord Basin may be suitable for safe and economically viable CO_2 storage. Given the lack of data on reservoir and seal properties, the approach chosen here is to carry out simulations applying a range of reservoir property parameters and to evaluate if a reasonable combination of these parameters yields a storage potential. If there exists a favourable parameter combination, it may be worth to make more detailed investigations, such as to drill an exploration well, determine the lithology in the basin, and to measure reservoir properties of rocks in the subsurface of the Beitstadfjord. If there is no suitable parameter combination, the conclusion could be that this site is not suitable for underground CO_2 storage.

The conditions to be fulfilled for suitablility of this site were:

- only minor leakage of CO_2 during and after injection (yearly leakage rate lower than 0.01 % of the total injected CO_2),
- storage capacity for all or a large part of the emissions from a planned power station at Skogn (Figure 2), that is, up to a total of 50 million tonnes during 25 years of injection.[1]

4.2 An outline of major expected processes in the reservoir

CO_2 injected into the subsurface will at normal pressure-temperature conditions have a density lower than water. Depending on the temperature and pressure gradients there will be a transition from gaseous (low density) to 'super-critical' (high density, but still lower than water) CO_2 at a certain depth. Due to the density difference between water and CO_2, there will be buoyancy-driven upward migration of CO_2 from the perforated or open part of the injection well until it reaches a barrier for migration. Such barriers are typically low permeable rocks for which high capillary entrance pressures have to be overcome to allow CO_2 migration into it. CO_2 will then accumulate below the barrier and spread laterally below it. If there are permeable pathways through the barrier, they will be exploited and parts of the CO_2 will migrate upwards through them. If the barrier is inclined, the CO_2 will migrate below the barrier up-dip.

Some CO_2 will dissolve in formation water. This is however a slow process as compared to migration. The establishment of convection in the reservoir will improve dissolution (Lindeberg & Bergmo 2003)

If the formation into which CO_2 is injected is sealed completely, that is, if no formation water (and CO_2) can leave it (or at very slow rates compared to the CO_2 injection rate), pore pressure in the reservoir formation will increase. If the pore pressure in the formation or in its seal rises locally above a critical pressure, hydraulic fracturing will occur (see below). Pore pressure rise will be strongly governed by the ratio between volume injected CO_2 and available pore volume in the formation; the lower this ratio, the lower will be the pressure increase.

[1] After the reservoir simulations were carried out, a case of capture and storage of only 5% of the total produced CO_2 from the power station came into discussion . The case of an annual storage rate of 100 000 tonnes CO_2 and a total storage quantity of 2.5 million tonnes is addressed in the discussion chapter of this study.

In the Beitstadfjord case, the Quaternary cover is the main seal. If it is absent (areas of non-deposition or of complete erosion) above the subcrop of a reservoir formation and/or if its permeability is high, formation water will be able to leave the reservoir without becoming overpressured, but CO_2 will leak. If the Quaternary is tight or has very low permeability, injected CO_2 may be retained but injection will lead to pore pressure increase. In the case of local hydraulic fracturing of the Quaternary, pathways with probable high permeability are created through which CO_2 will escape.

Hydraulic fracturing – maximum pore pressure condition

Hydraulic fracturing occurs when the minimum effective principal stress becomes smaller than the tensile strength of the material. The minimum effective principal stress is the minimum principal stress minus pore pressure. The condition to be fulfilled to avoid hydraulic fracturing is thus:

$$\sigma_3 - P_p \geq \sigma_T$$

where σ_3 is minimum pricipal stress, P_p is pore pressure, and σ_T is tensile strength.

In the Beitstadfjorden case, the maximum principal stress is probably the vertical stress (lithostatic stress, σ_v) and the minimum principal stress is accordingly the smallest horizontal stress (σ_h). A typical relationship between the vertical stress and the horizontal stress in such cases is

$$\sigma_h = c \cdot \sigma_v$$

where c is a constant and the vertical stress is

$$\sigma_v = \int_0^Z (\rho(z) \cdot g) dz$$

where Z is the depth for which vertical stress is calculated and ρ is the bulk rock density as a function of depth z.

The constant c is often taken to be of the order of 0.7 to 0.85 (e.g. Twiss & Moore 1992, Bjørlykke 1999). Here, an optimistic value of 0.85 was chosen.

Tensile strength σ_T is a material-specific parameter. For uncemented rocks such as the Quaternary in the Beitstadfjorden, tensile strength is 0 (zero).

For an average water depth above the subcrop of the relvant formation ('Ile' Formation) of approximately 100 m, an average thickness of the Quaternary of 75 m, a water density of 1010 kg/m^3, and an estimated bulk density of the Quaternary of approximately 2000 kg/m^3, this yields a possible overpressure of approximately 0.36 MPa or 3.6 bar.

4.3 Reservoir model and input data

Reservoir model

Based on the geological concept for the Beitstadford Basin and the analysis of the available data on its sedimentary infill as presented in Chapter 3, a reservoir model has been generated (Figure 13) using the Irap RMS software package.

This model assumes two formations with suitable reservoir properties for CO_2 storage: the upper parts of seismic units C and B, for simplicity being termed 'Ile Formation' and 'Garn Formation', respectively (Table 2). The lower parts of seismic units C ('Ror Formation') and B ('Not Formation') and seismic unit A ('Melke Formation') are assumed to be tight. All these formations are tilted with a general dip towards NW.

The tilted formations are discordantly overlain by a Quaternary cover. The interpolated bathymetry and the base Quaternary horizon suggest a very thin or absent Quaternary succession in an area in the southeast (Figure 6), above the subcrop of the 'Ile Formation'. Possible 'holes' in the Quaternary succession may be artefacts due to the interpolation procedure for the horizons but anyhow the thickness of Quaternary deposits in this area is low. For a few simulations these 'holes' were treated as open, and for most simulations they were treated as covered by a thin layer of Quaternary to test the effect on simulation results. The thickness of the Quaternary above all the subcrop area of the 'Ile Formation' is low (generally below 50 m).

The whole subcrop area of the 'Garn Formation' is covered by Quaternary deposits, which are there much thicker (50-150 m) than over the 'Ile Formation'.

The seawater above the Quaternary cover was represented by a layer of cells with 100% porosity and very large volume, thereby simulating a large capacity for formation water or CO_2 migrating upwards from the basin.

The basement below the sedimentary succession is not included in the reservoir model. It is thus treated as impermeable.

Table 2 Seismic units, formations, and their status in simulations

Seismic unit	C	C	B	B	A	-	-
Formation/ Subgrid	'Ror'	'Ile'	'Not'	'Garn'	'Melke'	Quaternary	Water
Status in simulations	Inactive	Active	Inactive	Active	Inactive	Active	Active

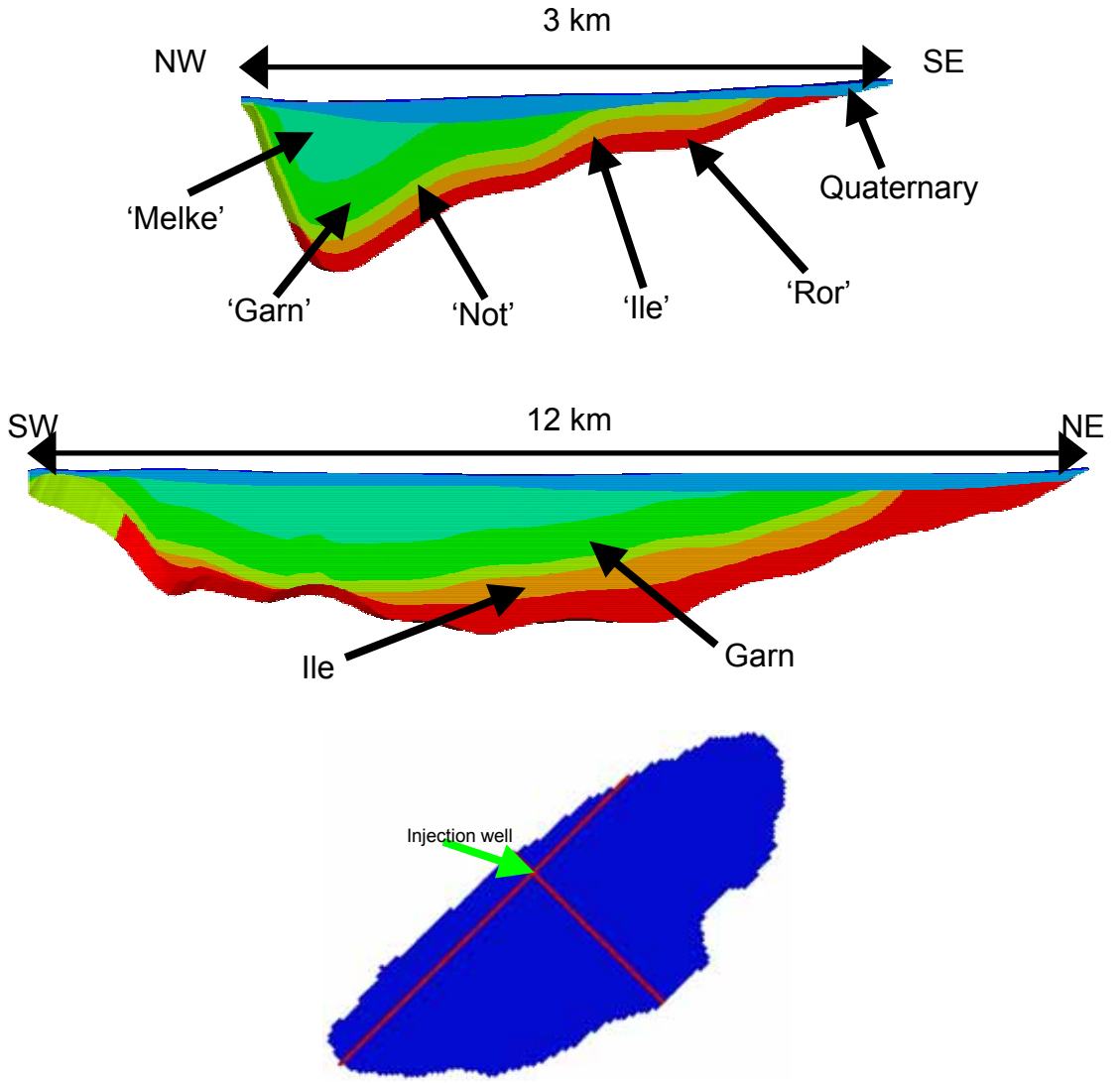

Figure 13 *Cross-sections through the reservoir model of the Beitstadfjord Basin and schematic map of the reservoir model showing their location. The formation colour code is identical in the two cross-sections. Seawater above the Quaternary is shown as thin dark blue layer.*

The reservoir model was constructed in the Irap RMS software package. The primary input for reservoir geometry were four horizons from seismic interpretation (bathymetry = top Quaternary, base Quaternary, top of seismic unit C = top 'Ile', and top basement = base of seismic unit C). Three additional horizons (top 'Ror', top 'Not', top 'Garn') were calculated by interpolation. Thickness ratios (Table 3)were based on averages from reported thicknesses of the offshore analogs of the formations. The horizons define seven formations or subgrids (Table 2): six sediment/rock formations (Figure 13) and a water layer on top. Subgrids with tight formations were treated as inactive. Lateral cell boundaries were always vertical. Cell dimensions were approximately 123 m in NE-SW direction and approximately 113 m in NW-SE direction. The final model consists of 66720 active cells. The reservoir properties (see below) are constant within each subgrid.

Table 3 Construction parameters for cells in the modelled formations in the subsurface geology model (Irap RMS).

'Formation'	Seismic unit	Thickness	Internal geometry	Number of active cells
Water	- -	Bathymetry	1 layer, parallel to base	4851
Quaternary	Quaternary	Quaternary	5 layers of constant relative thickness	24125
'Melke'	A	0.44 of (A + B)	none	inactive
'Garn'	A and B	0.42 of (A + B)	25 m thick cells, parallel to base	18857
'Not'	B	0.14 of (A + B)	none	inactive
'Ile'	C	0.4 of C	20 m thick cells, parallel to base	18887
'Ror'	C	0.6 of C	none	inactive

Reservoir properties

Porosity and permeability of the formations in the Beitstadfjord Basin are only poorly constrained due to the lack of samples. Based on the arguments given in Chapter 3, using analogy to the formations in hydrocarbon fields of the continental shelf offshore Mid-Norway, a range of parameters has been applied to the formations (Table 4). Base case values are similar to those reported in Ehrenberg (1990) and Koch & Heum (1995). The likely range for glacial Quaternary deposits is 0.0001 to 0.1 mD. These values, their harmonic mean (0.00316 mD), tight Quaternary (0 mD) and some values to test the effect of permeable Quaternary deposits (10 mD and 1000 mD) were used.

Table 4 Reservoir parameter range applied to the formations in the Beitstadfjord Basin

Formation	Net-to Gross ratio	Net porosity	Net horizontal permeability [mD]
Quaternary	1	20%	0 (tight), 0.0001, 0.00316, 0.1, 10, 1000
'Melke Formation'	0 (inactive)	0 (inactive)	0 (inactive)
'Garn' Formation	0.75	25% (base case), 12.5%	2000 mD (base case), 20 mD
''Not Formation'	0 (inactive)	0 (inactive)	0 (inactive)
'Ile Formation'	0.75	25% (base case), 12.5%	2000 mD (base case), 20 mD
'Ror Formation'	0 (inactive)	0 (inactive)	0 (inactive)

Vertical heterogeneity within the formations was represented by a ratio of 0.1 between vertical and horizontal permeability (k_v and k_h respectively).

No dependency of saturation to capillary pressure was assumed. Accordingly the entry pressure of CO_2 into reservoir and seal rocks is 0.

Reservoir conditions

A seawater temperature of 8° C was assumed. This corresponds accordingly to the temperature at the sea floor, which is on average at approximately 150 m bsl. Temperature measurements at the Malm mines a few km north of the Beitstadfjord yielded 29° C at 1200 m b.s.l. (A. Myrvang, pers. comm. 2003). The temperature gradient is accordingly 20° C/km (Figure 14).

Pore pressure at injection start was assumed to be hydrostatic (Figure 14).

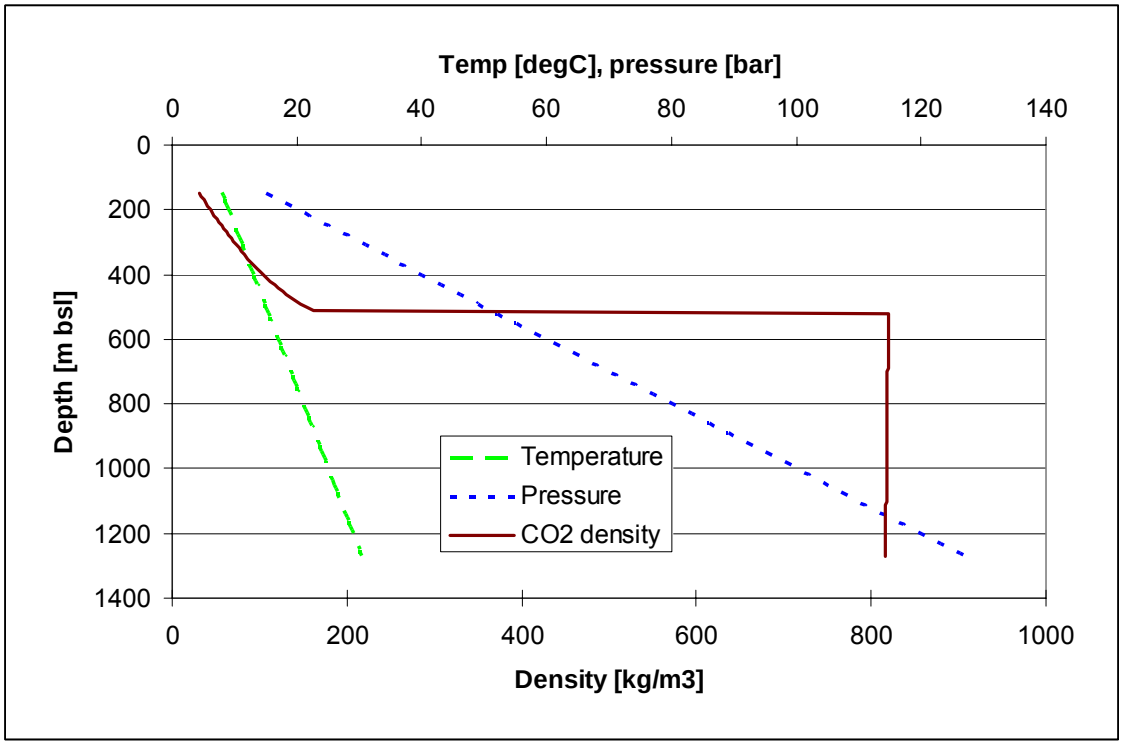

Figure 14 *Calculated temperature, pressure and CO_2 density versus depth for the Beitstadfjord Basin.*

Fluid properties

Density and viscosity of water and CO_2 was calculated using SINTEF's thermodynamic model for the CO_2-CH_4-H_2O system (Lindeberg et al. 2000). The density variation with depth for the calculated temperature and pressure profiles is shown in Figure 14. The major feature of interest is the strong downward density increase at approximately 500 m b.s.l., below which CO_2 density is higher than 800 kg/m^3.

Figures illustrating the variation of water density with pressure and the dependency of viscosity on pressure and temperature are provided in Figure 15, Figure 16, and Figure 17.

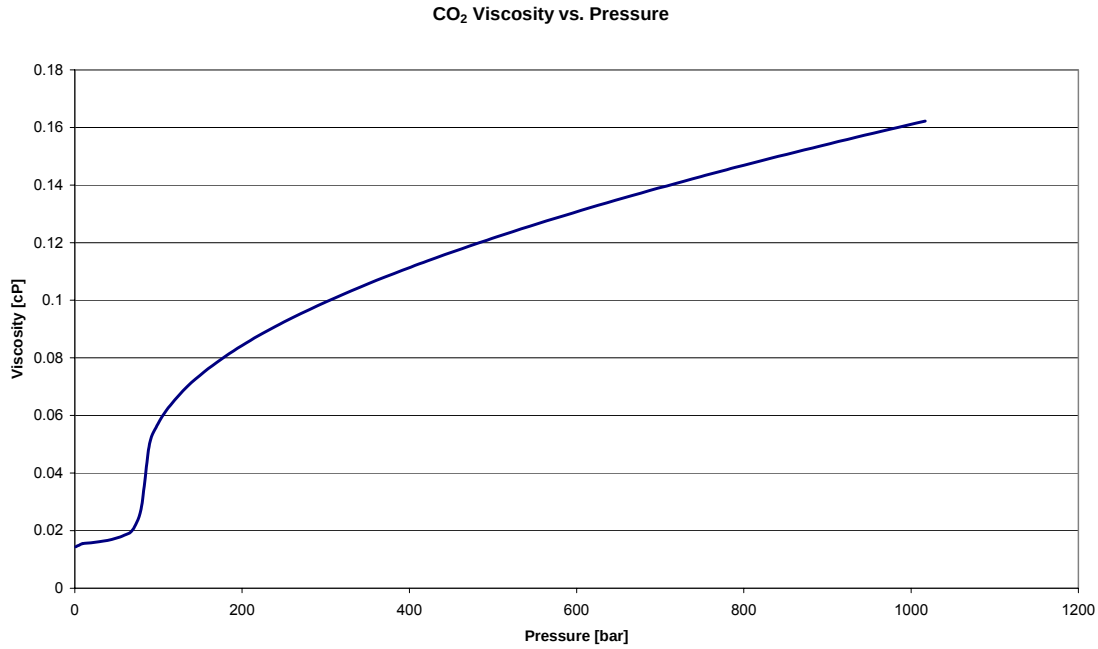

Figure 15 CO_2 viscosity vs. pressure at reservoir temperature of 31°C

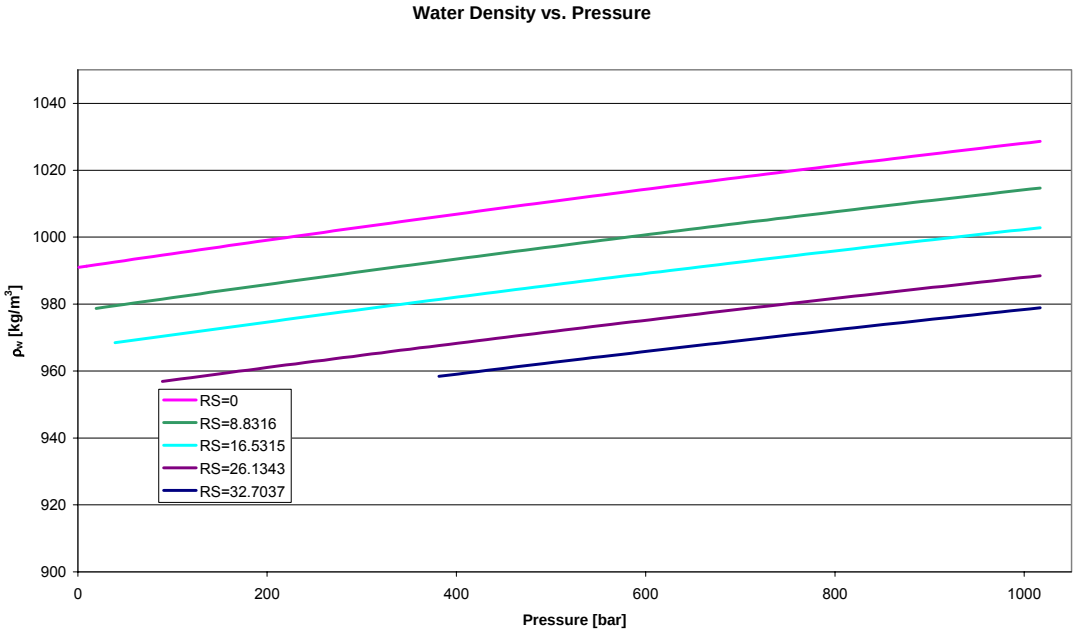

Figure 16 Density of reservoir water at different CO_2 saturation vs. pressure at reservoir temperature of 31°C

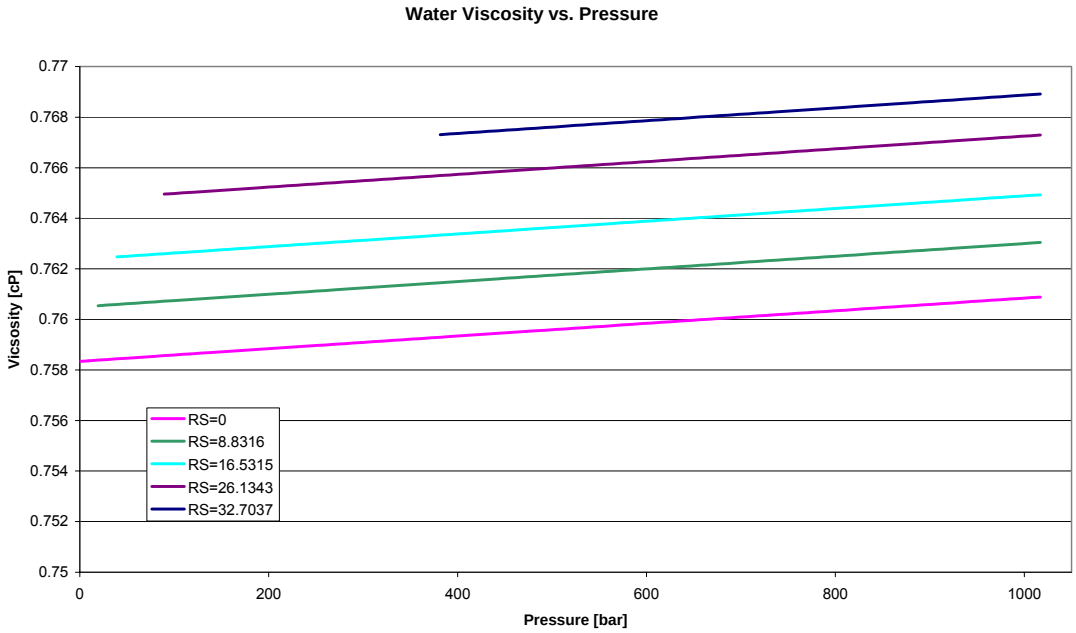

Figure 17 *Viscosity of reservoir water at different CO_2 saturation vs. pressure at reservoir temperature of 31^oC*

Relative permeability curves used for water and CO_2 in the water-CO_2 system are shown in Figure 18. The curves for the cases with CO_2 permeability correspond to an irreducible water saturation of 0.3 and a residual CO_2 saturation in imbibition of 0.2. All relative permeability curves assume no hysteresis effects (same curves for drainage and imbibition).

In some simulation runs, the Quaternary was considered as permeable for water (though with low absolute permeability) but impermeable for CO_2. The relative permeabilities in these runs are 1 for water and 0 for CO_2.

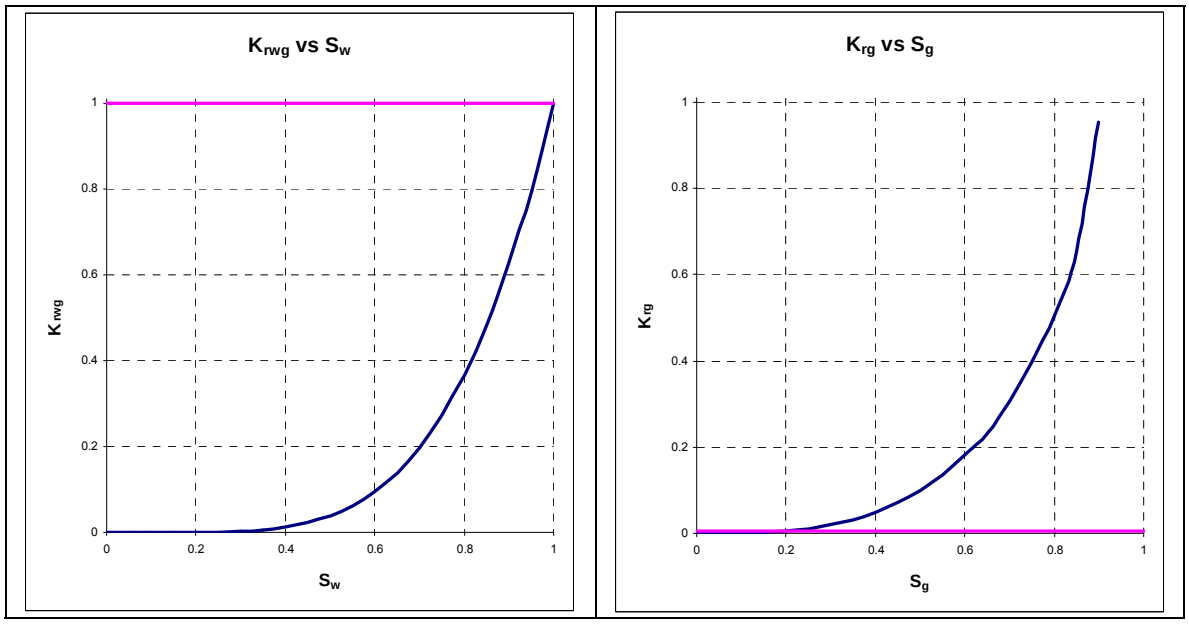

Figure 18 *Relative permeability curves for water (left) and CO_2 (right). Pink curves are for simulation runs treating Quaternary as permeable for water but impermeable for CO_2.*

Calculated reservoir volume

The constructed reservoir model had for the base case of a Net-to-Gross ratio of 0.75 and a net porosity of 25% the volumes listed in Table 5.

Table 5 Calculated reservoir volumes (in Eclipse) in 10^6 m^3

Formation	'Ile'	'Garn'
Bulk volume	4372	5745
Total pore volume	820	1077

Other simulation specifications

Reservoir simulation was carried out with the commercial 'Eclipse 100' black-oil simulator.

Wells were treated as vertical. In the case of simultaneous co-injection, two parallel wells at the same location were assumed to facilitate individual steering of injection rates. The well positions and perforations for injection are placed at positions that are expected to result in the longest migration path to the surface, that is where the reservoir formations have their deepest position in the basin and the perforations are immediately above the base of the storage formations.

The injection rate was defined as 2 million tonnes/year which corresponds to 2930188.26 Sm^3/day and a total of 26.7 10^9 Sm^3. In the cases of contemporaneous injection into both the

'Ile' and 'Garn' formations, the injection rate was divided proportionally to the available pore volume (Table 5), that is in a ratio of 1 : 1.313 ('Ile' : 'Garn').

The diffusion option of the Eclipse software was not applied because the effect of diffusion is negligible in short term simulations.

Most simulations were run for 50 years, that is until 25 years after the end of simulated injection.

4.4 Simulation results

Simulations are grouped into two major sets:

- cases with low-permeable seal in which the permeability of the Quaternary succession is 0.1 mD or lower and in which for most cases the Quaternary is tight for CO_2
- cased with high-permeable seal in which the permeability of the Quaternary succession is 0.1 mD or higher and in which the Quaternary is permeable for CO_2

For the former set, pressure build-up in the reservoir will be the central issue, whereas for the latter set leakage rates are more critical.

4.4.1 Low-permeable Quaternary seal cases

In this set of simulations seal permeability (that is, the permeability of the Quaternary sediments) is assumed to be low. Three main groups of cases have been investigated:

- Simultaneous co-injection into both 'Ile' and 'Garn' formations
- Injection into 'Ile Formation' only.
- Injection into 'Garn Formation' only.

All groups of cases with a low-permeable Quaternary seal have been simulated for four different permeabilities of the Quaternary (Table 6). The entry pressure for CO_2 with respect to the Quaternary was assumed to be very high, that is relative permeability for CO_2 was always assumed to be 0. Reservoir net-to-gross ratio, net porosity and net permeability were in all these cases constant and with optimum values (Table 6) to yield the largest possible available pore space.

No hydraulic fracturing of the seal has been included in the simulations. The seal is assumed to remain intact in spite of overpressure.

Table 6 Parameters used for simulations with low permeable Quaternary.

Parameter	Value
k_h in Quaternary [mD]	0 0.0001 0.00316, 0.1
Injection rate [Sm^3/day]	
Single formation	2930188.26
Co-injection, 'Ile' part	1266150.37
Co-injection, 'Garn' part	1664037.89
Quaternary permeable for	Water only
Injection time [years]	25
Net porosity in reservoir	0.25
k_h in reservoir [mD]	2000
k_v in reservoir [mD]	200
NTG in reservoir	0.75

kh = horizontal permeability, kv = vertical permeability,
NTG = net-to-gross ratio

Estimate of maximum injectible volume from the hydraulic fracturing condition

A rough estimate of the maxuimum volume of CO_2 that can be injected into the combined volume of the 'Ile' and 'Garn' formations while remaining below a critical average reservoir pressure has been calculated. The principle of the calculations is that injected CO_2 will require pore space and that it will compress formation water and the rock matrix. Larger injected CO_2 volumes will cause stronger compression of all three involved phases (CO_2, formation water, and rock matrix).

Two alternatives were considered:

- no dissolution of CO_2 in formation water
- saturation of formation water by dissolution of injected CO_2.

The latter is an extremely optimistic case, because dissolution is a slow process operating on a time scale of 100s or 1000s of years.

The results (Table 7, Figure 19) show that only very limited amounts of CO_2 can be injected if the reservoir pressure shall remain below the critical pressure of 3.6 bar. In case of no dissolution, which approximates the situation during injection, only 271 000 tonnes could be injected, which corresponds to 1.6 months at the planned rate of 2 million tonnes per year, or to 32.5 months at the reduced rate (5%) of 100 000 tonnes per year.

Table 7 Parameters and results for a rough estimate of maximum injectible CO_2 in the 'Ile' and 'Garn' formations. The pressure is kept below the critical pressure for hydraulic fracturing. 'M' in unit column is million.

Parameter	Unit	Value
Average reservoir temperature	C°	20
Average reservoir pressure, p_0 (prior to injection)	bar	70
Maximum pressure increase, Δp	bar	3.6
Average CO_2 density at p_0	kg/m^3	809
Average CO2 density at at (p_0 + Δp)	kg/m^3	816
Reservoir volume	Mm^3	10117
Net-to-gross ratio		0.75
Net porosity		0.25
Pore volume	Mm^3	1897
Max dissolved CO_2 @ saturation (50 kg CO_2 per m^3 water)	Mtonne	94.8
Density of brine@res press	kg/m^3	1027.8
Density of brine@res press + max increase	kg/m^3	1028.0
Max brine density increase	kg/m^3	0.154
Brine shrinkage from p_0 to (p_0 + Δp)	Mm^3	0.285
Rock compressibility	1/bar	0.0000016
Rock shrinkage from p_0 to (p_0 + Δp)	Mm^3	0.047
Maximum free CO_2 at (p_0 + Δp)	Mtonne	0.271
Total max CO_2 (dissolved & free) at (p_0 + Δp)	Mtonne	95.12

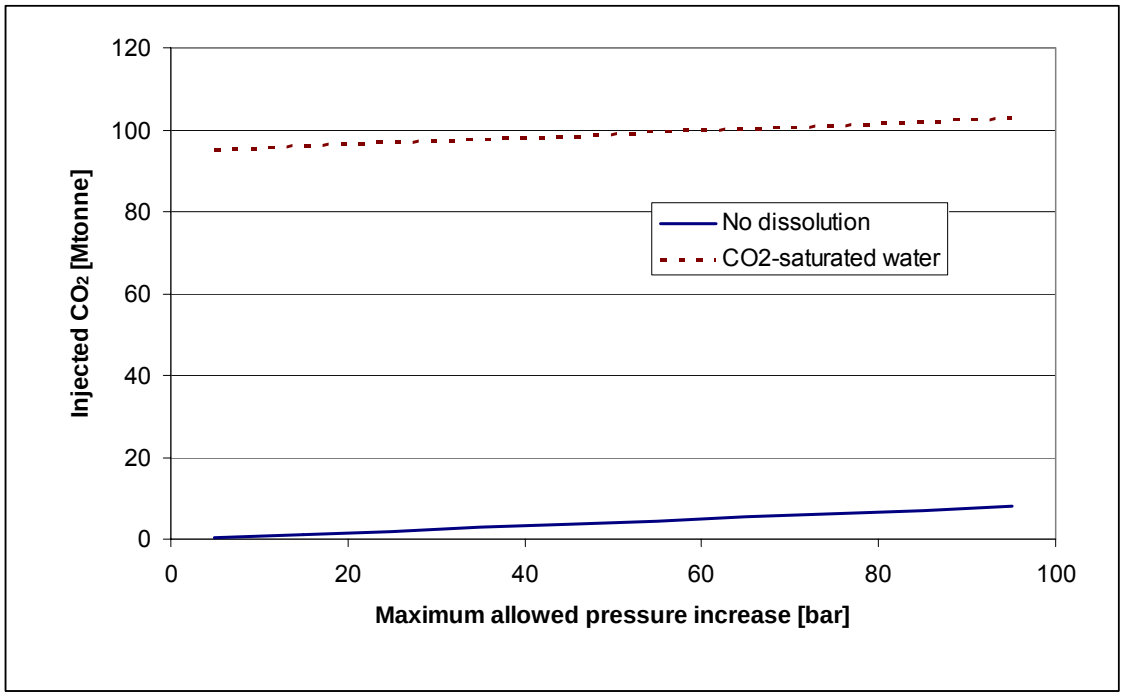

Figure 19 Maximum injectible CO_2 as a function of the critical pressure for hydraulic fracturing

Detailed simulation – co-injection into 'Ile' & 'Garn'

Simulated development of the average reservoir pressure through time for the cases of simultaneous CO_2-co-injection into both 'Ile' and 'Garn' formations is shown in Figure 20. It is evident from these graphs that the reservoir pressures would increase to far above the critical limit of approximately 3.6 bar after a short time for all chosen seal permeabilities. Note that the permeability of 0.1 mD for the most permeable case is already quite high, and is above the reservoir permeability of some producing 'tight gas' reservoirs. Pressures would in reality not increase to the levels simulated here, because hydraulic fracturing of the seal at an early stage would increase seal permeability dramatically, causing pressure release by water outflow and associated CO_2 leakage into the seawater.

Leakage volumes for the simulated cases with low permeable seal are shown in Figure 21. CO_2 could leak in spite of relative permeability for it being zero, because it was transported through the seal as dissolved gas in formation water. In the cases with seal permeability lower than 0.1 mD, no significant leakage occurred within the simulated 50 years. For the case of a seal permebaility of 0.1 mD the simulated cumulative leakage volume is very small, corresponding to 0.007% of the total injected volume, or the equivalent of the volume injected during about 16 hours.

A peculiarity of many of the simulated cases is that CO_2 at the simulated high pressures (above approximately 500 bars) becomes denser than water and migrates towards the base of the reservoir. It is than still a separate 'supercritical' phase and is not yet dissolved in water. This may partly explain the low leakage rates.

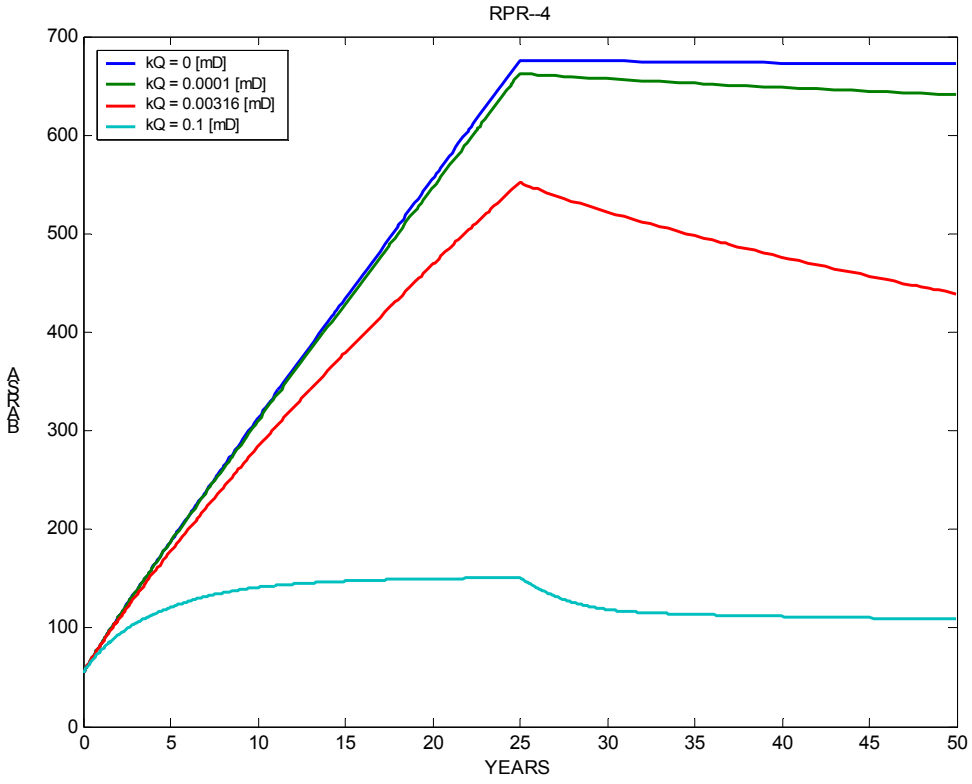

Figure 20 *Simulated average reservoir pressure for the case of co-injection into the 'Ile' and 'Garn' formations, for four different low seal permeabilities (kQ). Upper: in the 'Ile Formation'; lower: in the 'Garn Formation'.*

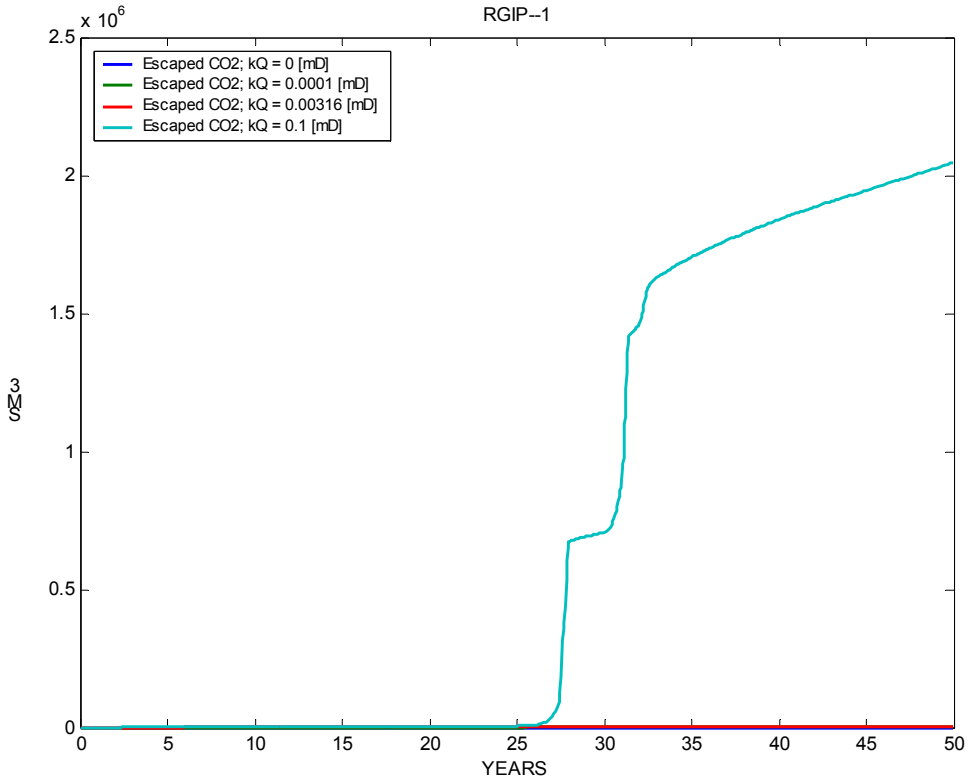

Figure 21 *Simulated cumulative volume of CO_2 leaked from the reservoirs for the case of co-injection into the 'Ile' and 'Garn' formations, for four different low seal permeabilities (kQ). All cases with kQ lower than 0.1 mD yielded no significant leakage during the simulated 50 years.*

Detailed simulation – injection into 'Ile' & 'Garn' separately

The cases of full injection into either the 'Ile Formation' or the 'Garn Formation' have also been simulated. They yielded even higher pressures than for the case of co-injection, which is due to the fact that the ratio between injected volume to available pore volume is higher. Similarly, simulated pressures for the 'Garn Formation' is lower than those for the 'Ile Formation', because the former has a larger available pore volume. Results of these simulations are presented in Figure 22 and Figure 23.

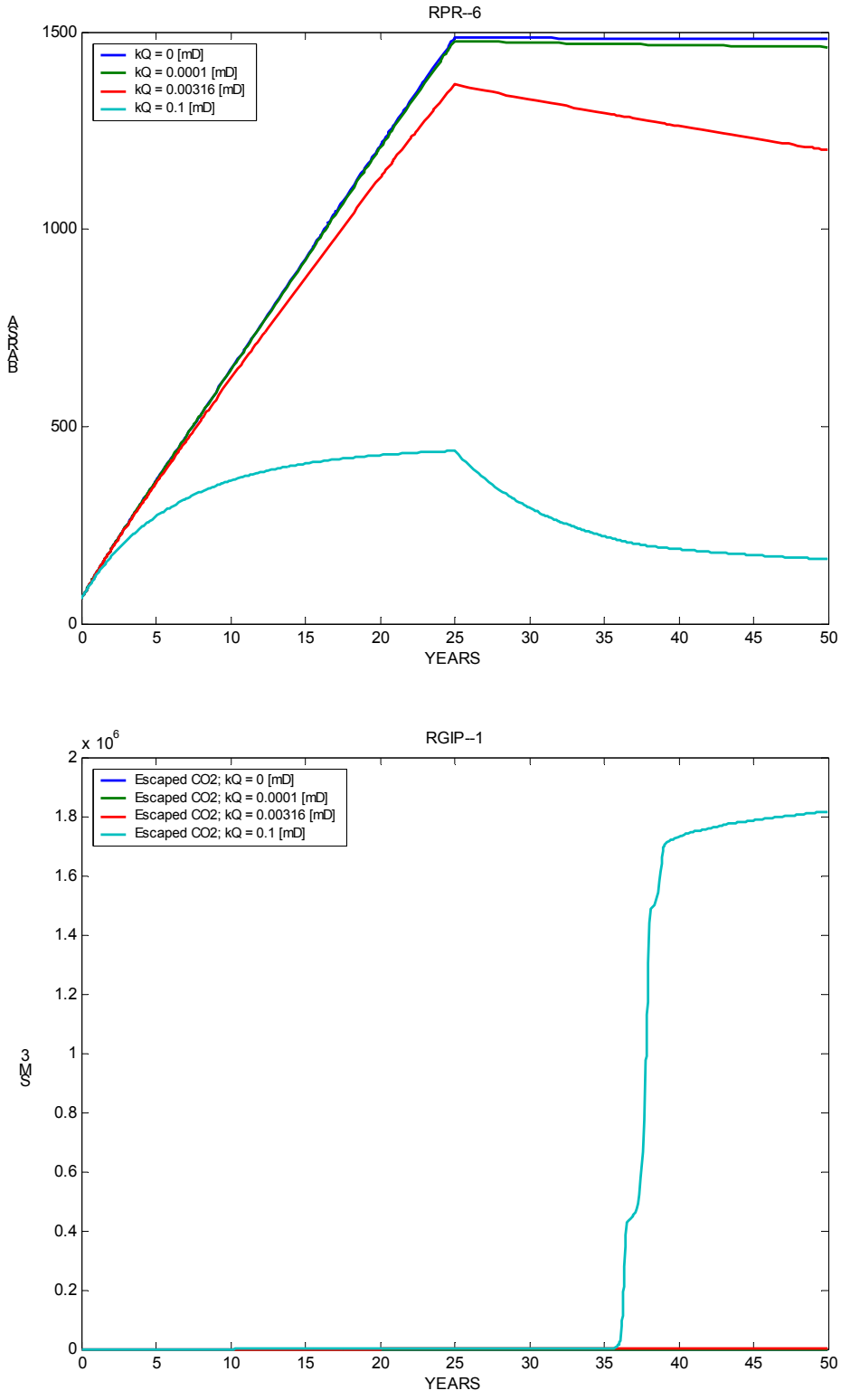

Figure 22 *Results of simulated cases of injection into the 'Ile Formation' only and for four different low seal permeabilities (kQ). Upper: simulated average reservoir pressure; lower: simulated cumulative volume of CO_2 leaked from the reservoir.*

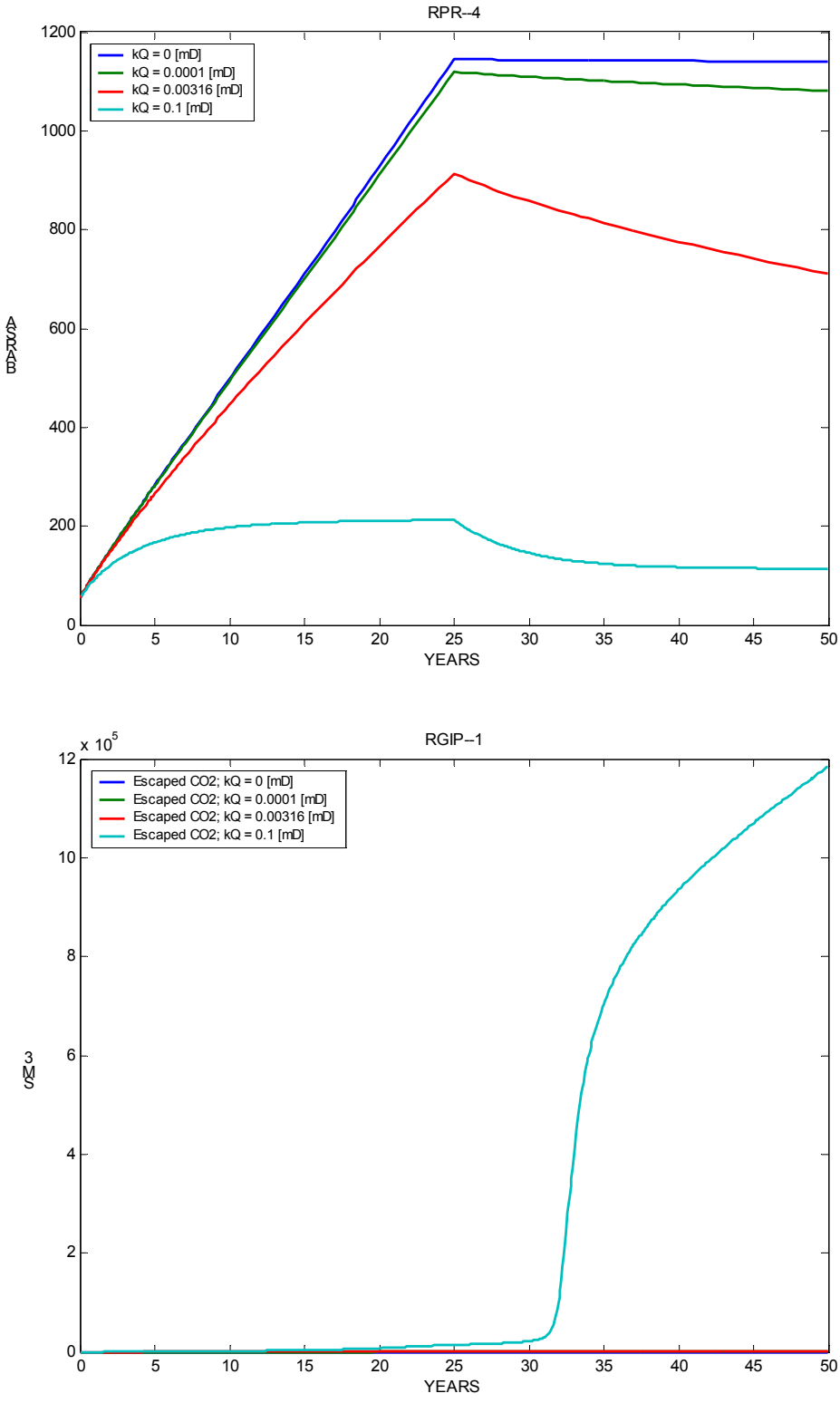

Figure 23 *Results of simulated cases of injection into the 'Ile Formation' only and for four different low seal permeabilities (kQ). Upper: simulated average reservoir pressure; lower: simulated cumulative volume of CO_2 leaked from the reservoir (note the scale of the vertical axis).*

4.4.2 High-permeable Quaternary seal cases

Simulations of this set can be grouped into five groups:

- Simultaneous co-injection into 'Ile' and 'Garn' formations with high reservoir permeability and porosity
- Simultaneous co-injection into 'Ile' and 'Garn' formations with reduced reservoir permeability and in one case also reduced reservoir porosity
- Injection into the 'Ile' Formation only.
- Injection into the 'Ile' Formation only assuming a 'hole' in the seal.
- Injection into the 'Garn' Formation only.

Detailed simulations – 'Ile' & 'Garn', high seal permeability base case

Simulated development of the average reservoir pressure through time for the cases of simultaneous CO_2-co-injection into both 'Ile' and 'Garn' formations below a high permeable seal is shown in Figure 24. Average pore pressure is predicted to increase initially and to decrease when CO_2 has started to leak from the reservoir. The average pore pressure will after injection end drop below the original reservoir pressure, which is caused by the replacement of water in the pore fluid column by CO_2 with lower density and the lack of active pressurization due to injection. Continued leakage of buoyancy-driven CO_2 (aided by minor dissolution) causes the fraction of CO_2 in the pore fluid column to decrease. The average density increases thus, and average pore pressure rises.

Maximum average pore pressure increase in the 'Ile Formation' in the case of a seal permeability of 10 mD is approximately 12 bars, which is higher than the critical limit to avoid hydrofracturing. For the 'Garn Formation' the maximum increase is approximately 5 bars which may be acceptable. If only 5% of the planned CO_2 emission from a power station would be injected, the pressure increase in none of the two formations would reach the limit of maximum 3.6 bars

Calculated leakage rates for the high permeable Quaternary cases are shown in Figure 25. This figure illustrates that very large proportions of the injected CO_2 would leak: after 50 years approximately 76% with kQ = 10 mD and approximately 89% with kQ = 1000 mD would have leaked into the sea water (and possibly partly into the atmosphere).

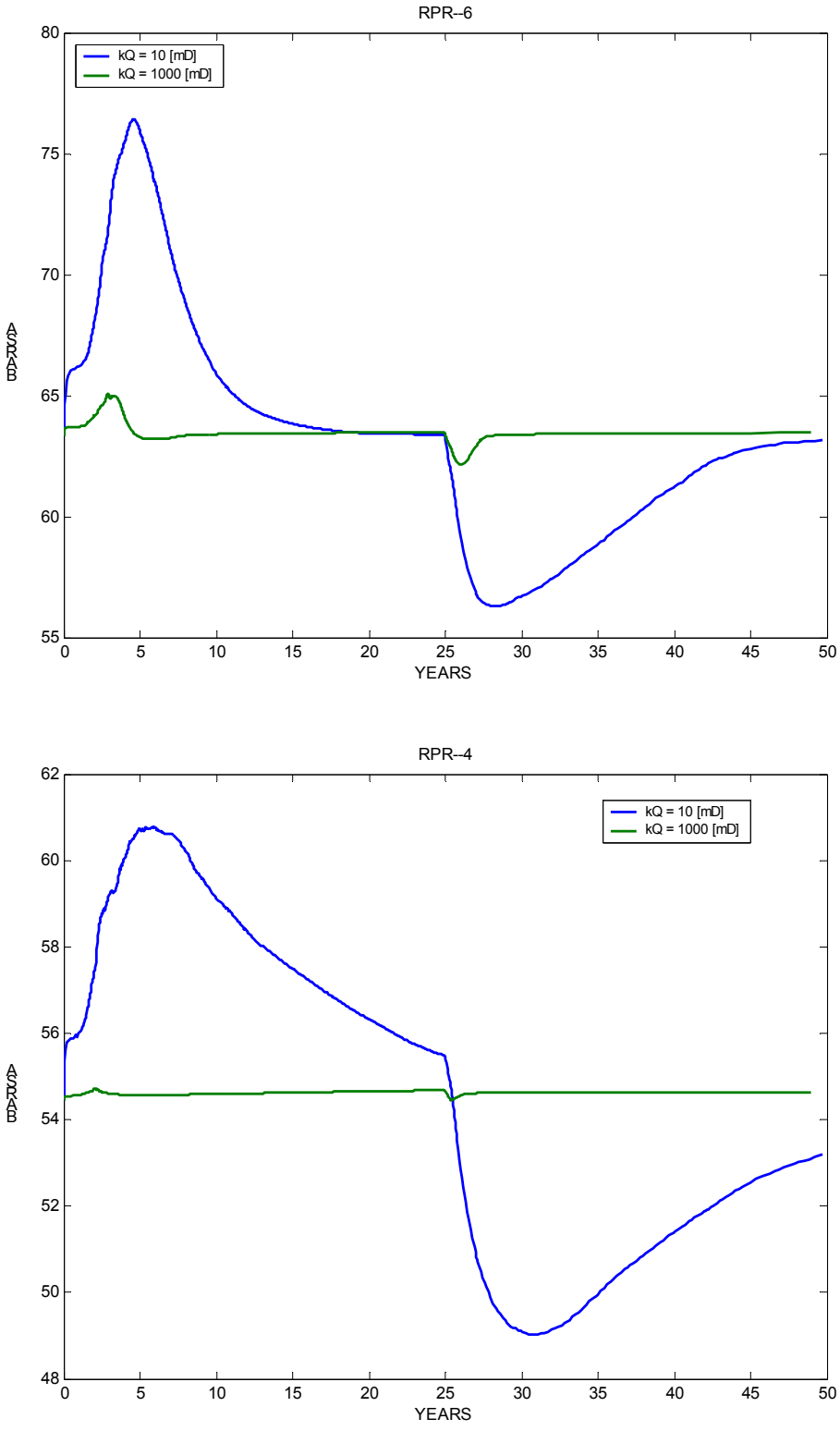

Figure 24 *Simulated average reservoir pressure for the case of co-injection into the 'Ile' and 'Garn' formations, for two different high seal permeabilities (kQ). Upper: in the 'Ile Formation'; lower: in the 'Garn Formation'.*

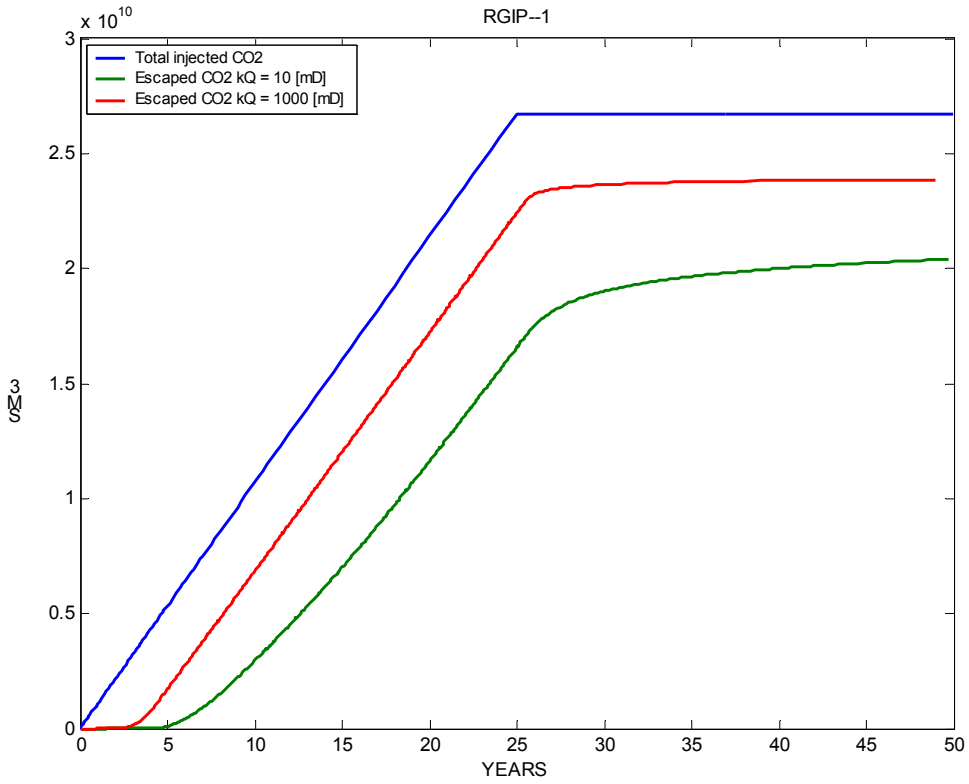

Figure 25 *Simulated cumulative volume of CO_2 leaked from the reservoirs for the case of co-injection into the 'Ile' and 'Garn' formations, for two different high seal permeabilities (kQ). The cumulative injected volume of CO_2 is also shown.*

Detailed simulations – 'Ile' & 'Garn', lower permeability and porosity of the reservoir

High leakage rates - as simulated for the base case with a high permeability seal – require high permeability of the reservoir formation. In the base case, reservoir permeability was assumed to be rather high, k_h being 2000 mD. As an alternative, a case with a lower reservoir permeability of k_h = 20 mD was simulated. However, reduced permeability is in general associated with a reduced porosity. Therefore a further case was simulated in which both reservoir permeability and reservoir porosity were reduced (kh = 20 mD, net poro = 12.5 %). Porosity reduction reduces the available pore space and will thus cause a higher pressure.

Results of these simulations are illustrated in Figure 26 and Figure 27. Average pore pressure (Figure 26) would rise to much higher levels than in the base case (blue curve) and would be much above the critical acceptable pore pressure. The leakage rates (assuming no hydraulic fracturing of the seal to occur in spite of high pore pressure) are smaller than in the base case (Figure 27), leading to a cumulative leaked volume of 5.5% of the total injected volume for the case with kh = 20 mD and net porosity = 25%, and 15.5% for the case with net reservoir porosity reduced to 12.5%, all of them at 50 years after injection start. Longer term simulations over 500 years show, however, that leakage in the low permebaility reservoir cases still would be high, being 72% of the total injected volume for the reservoir with 12.5% net porosity and 59% for the reservoir with 25% net porosity.

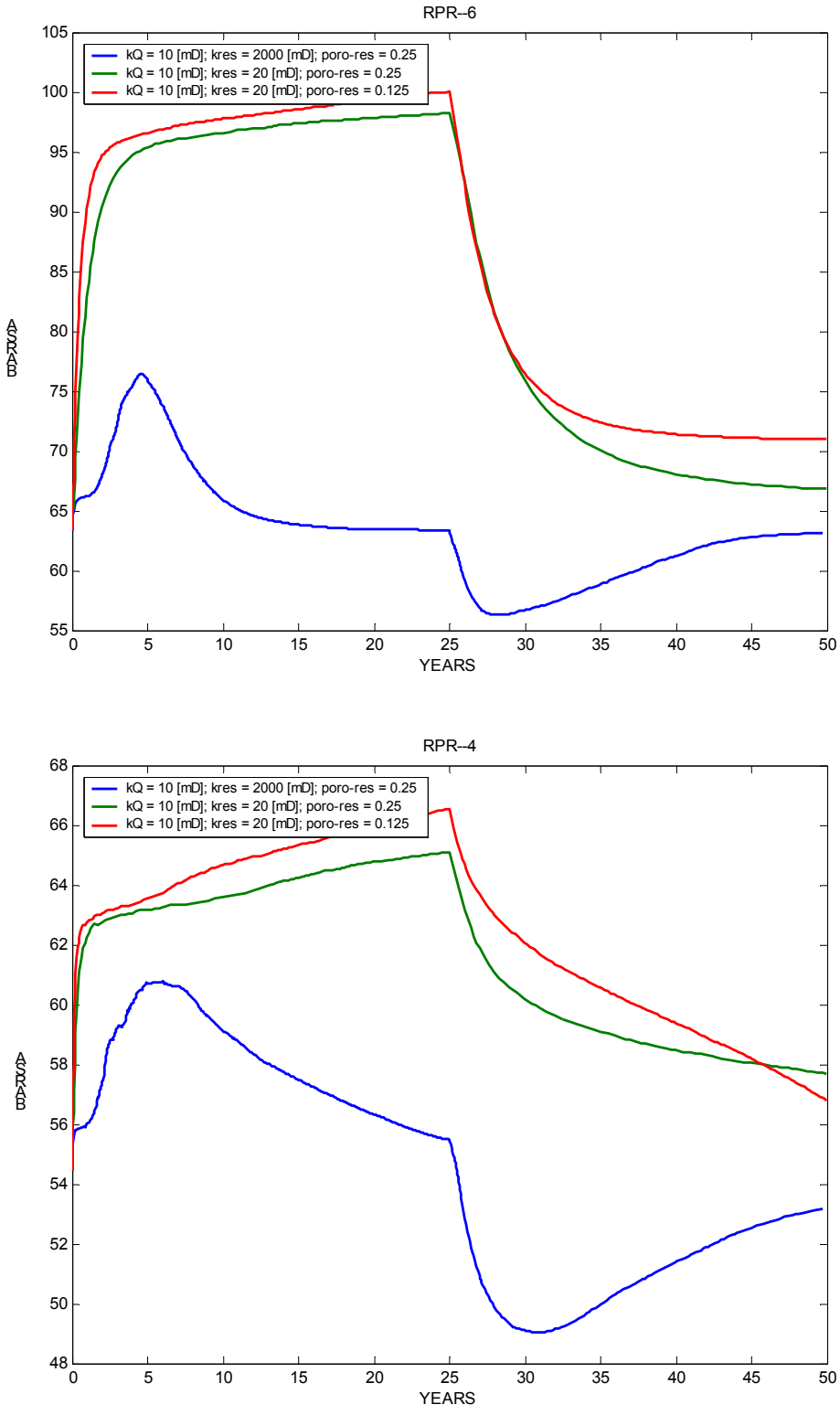

Figure 26 *Simulated average reservoir pressure for the case of co-injection into the 'Ile' and 'Garn' formations, for three combinations of high seal permeabilities (kQ) with reservoir permeability and net reservoir porosity. Upper: in the 'Ile Formation'; lower: in the 'Garn Formation'.*

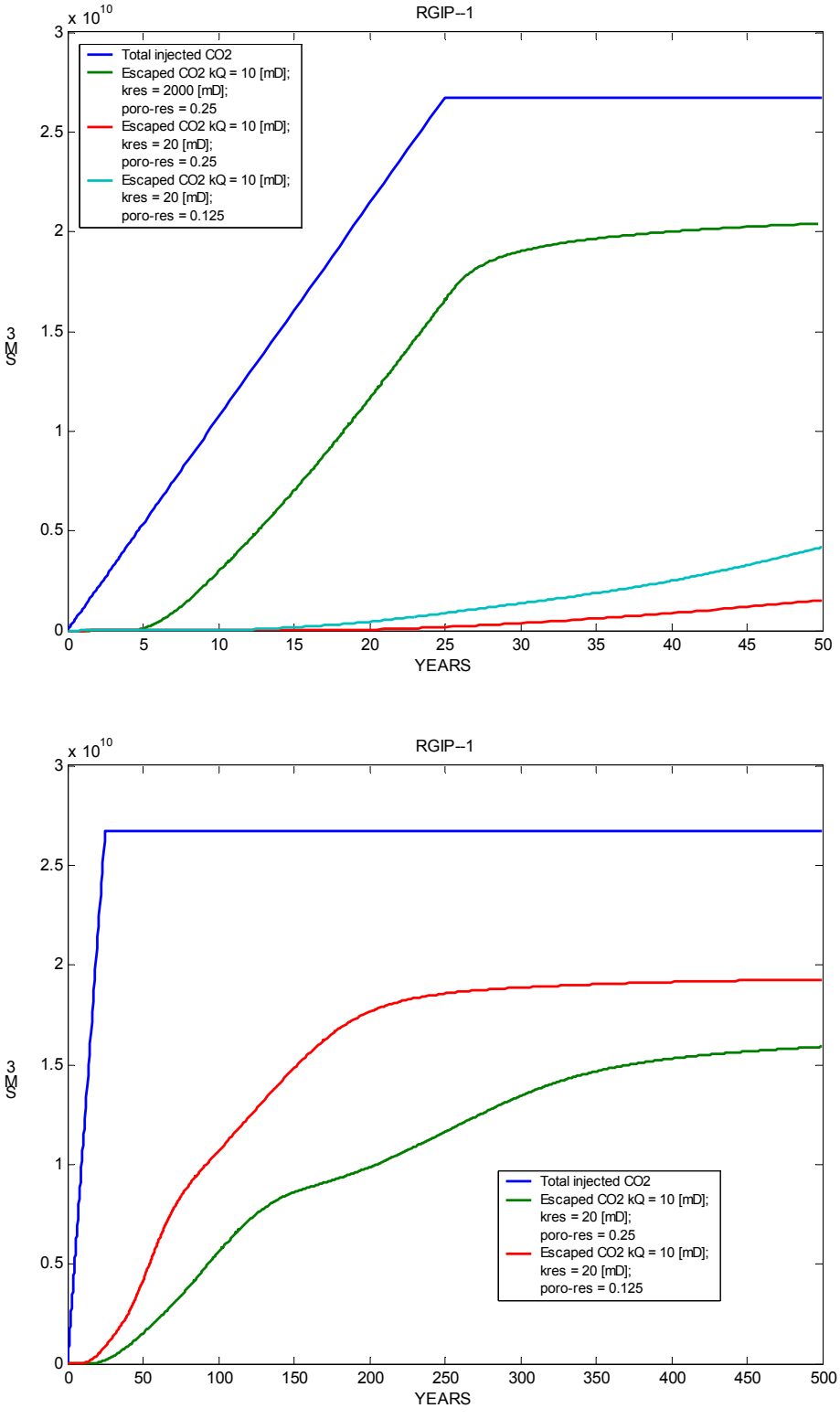

Figure 27 *Simulated cumulative volume of CO_2 leaked from the reservoirs for the case of co-injection into the 'Ile' and 'Garn' formations, for three combinations of high seal permeabilities (kQ) with reservoir permeability and net reservoir porosity. The cumulative injected volume of CO_2 is also shown. Upper: first 50 years from injection start; lower: first 500 years (two cases only) .*

Detailed simulations – Injection into 'Ile' only

Injection into only one formation may be somewhat cheaper than simultaneous injection into two formations, due to reduced drilling costs. The effect of injection in this case was tested by simulation of injection into the 'Ile' Formation only.

The simulation results show that pressure increase (Figure 28) will be too high with the exception of a very permeable seal (kQ = 1000 mD). However, simulated leakage rates (Figure 29) are for all cases too high, particularly for the cases with high seal permeability (more than 90% of the total injected volume leaked after 50 years) but also for the case of a relatively low seal permeability (approximately 13% leaked after 50 years).

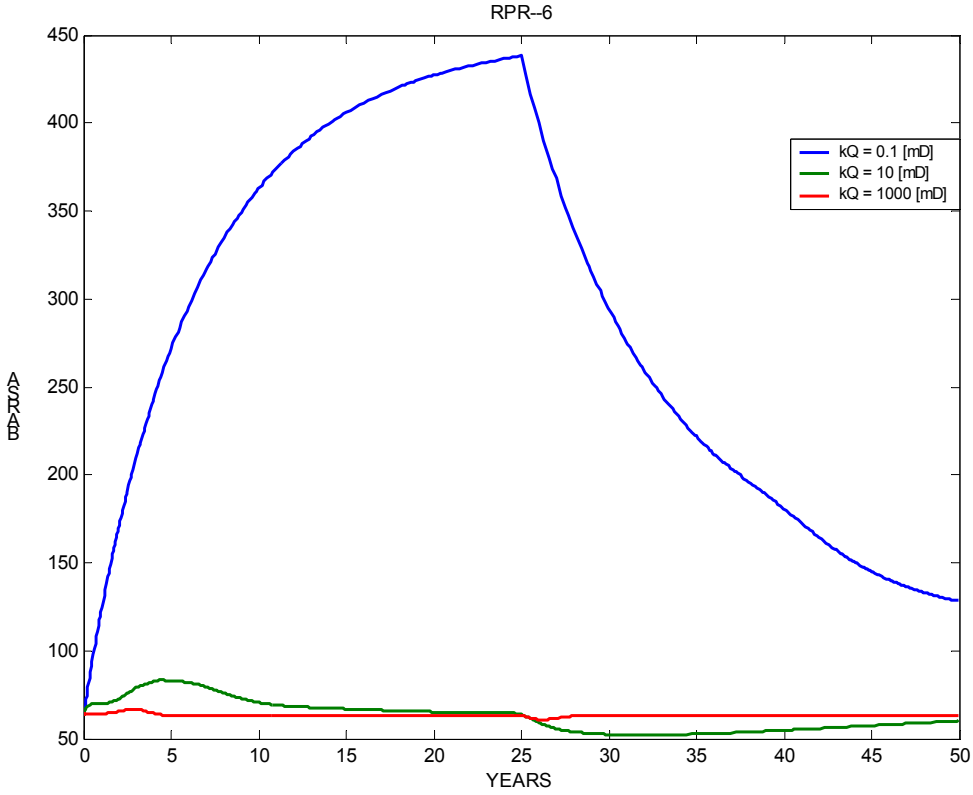

Figure 28 *Simulated average reservoir pressure for the case of injection into the 'Ile' Formation only, for three different high seal permeabilities (kQ).*

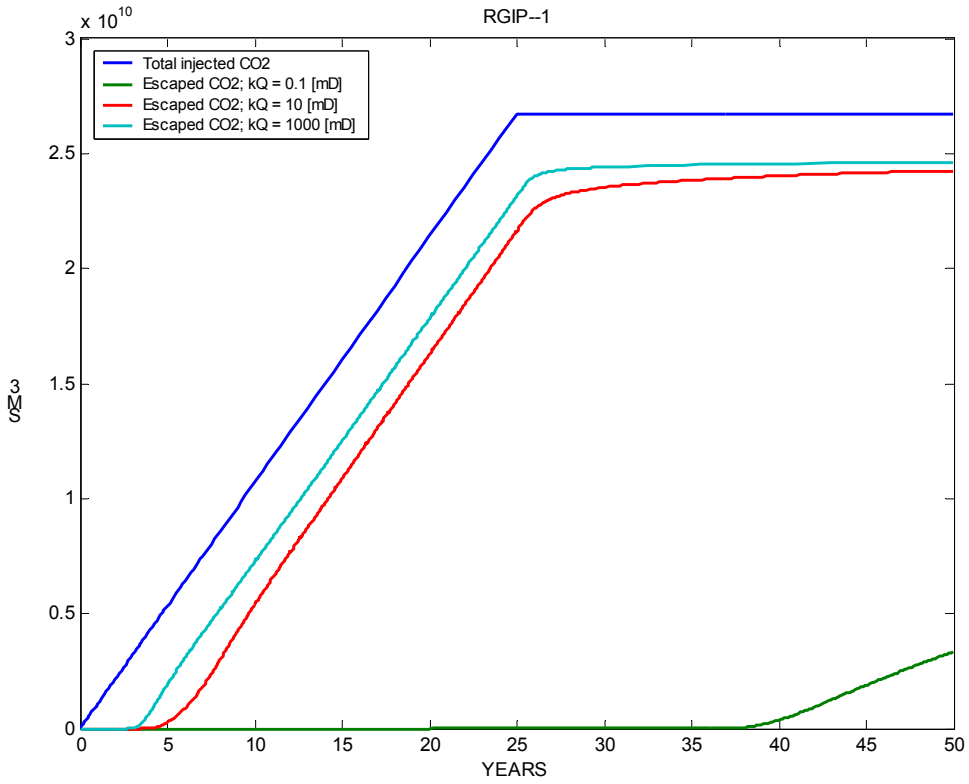

Figure 29 *Simulated cumulative volume of CO_2 leaked from the reservoir for the case of injection into the 'Ile' Formation only, for three high seal permeabilities (kQ).The cumulative injected volume of CO_2 is also shown.*

Detailed simulations – Injection into 'Ile' only; Quaternary seal has a 'hole'

In this case, the mapped 'hole' in the Quaternary was not closed, such that there was a direct, unsealed contact between the reservoir and the seawater. A variety of cases with variable seal permeabilities have been simulated.

The simulation results show that for cases with widely variable seal permeabilities the 'hole' in the seal has a very strong effect and the results are all extremely similar (Figure 30, Figure 31). Pressure increase (Figure 30) will be slightly above the acceptable limit, and in fact it may locally, at the base of the seal, be below the critical limit. However, simulated leakage rates (Figure 31) are for all cases too high, being approximately 90% of the total injected volume leaked after 50 years.

Simulated pressure decreases after 5 years towards and even below the initial reservoir pressure is caused by the replacement of water in the fluid column by CO_2 with lower density.

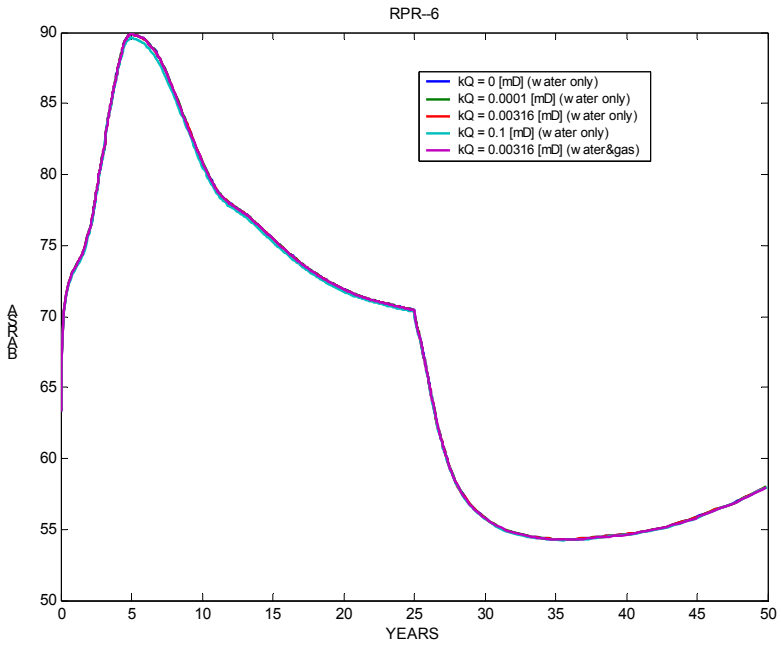

Figure 30 *Simulated average reservoir pressure for the case of injection into the 'Ile' Formation only with a hole in the seal (Quaternary), for five different seal permeabilities (kQ, relative permeability for water and gas).*

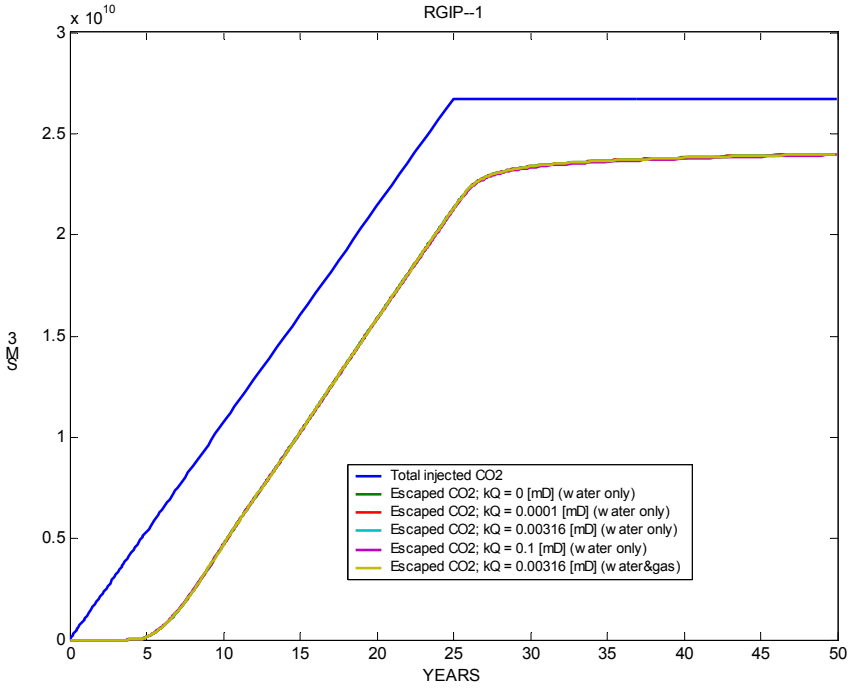

Figure 31 *Simulated cumulative volume of CO_2 leaked from the reservoir for the case of injection into the 'Ile' Formation only with a hole, for five different seal permeabilities (kQ, relative permeability for water and gas).The cumulative injected volume of CO_2 is also shown.*

Detailed simulations – Injection into 'Garn' only

Similarly as for the 'Ile' Formation the effect of injection into the 'Garn' Formation only case was tested by simulation. Based on the experience from the 'Ile only' cases (very high reservoir pressure at relatively low seal permeability), simulations were only run for high seal permeabilities (10 mD, 1000 mD).

The simulation results show that pressure increase (Figure 32) will be slightly too high for the case of kQ = 10 mD and would be acceptable for kQ = 1000 mD. However, simulated leakage rates (Figure 33) are for both cases much too high, being more than 90% of the total injected volume leaked after 50 years for the case of kQ = 1000 mD, and approximatley 76% for the case of kQ = 10 mD

Simulated pressure decrease after 5 years towards and even below the initial reservoir pressure is caused by the replacement of water in the fluid column by CO_2 with lower density.

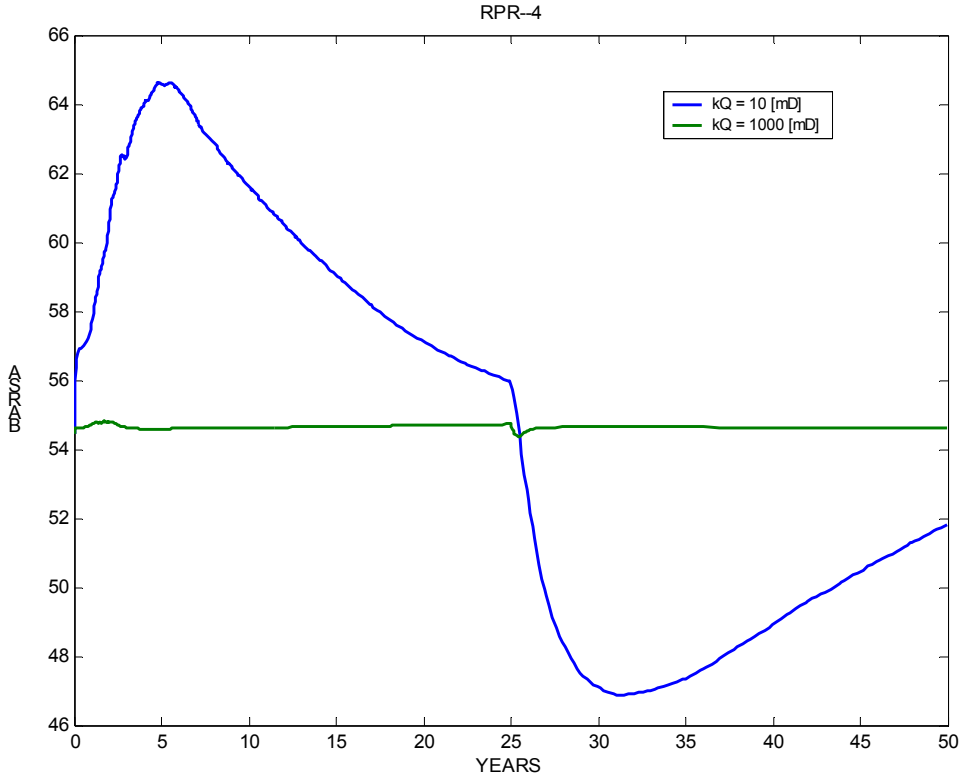

Figure 32 *Simulated average reservoir pressure for the case of injection into the 'Garn' Formation only, for two different high seal permeabilities (kQ).*

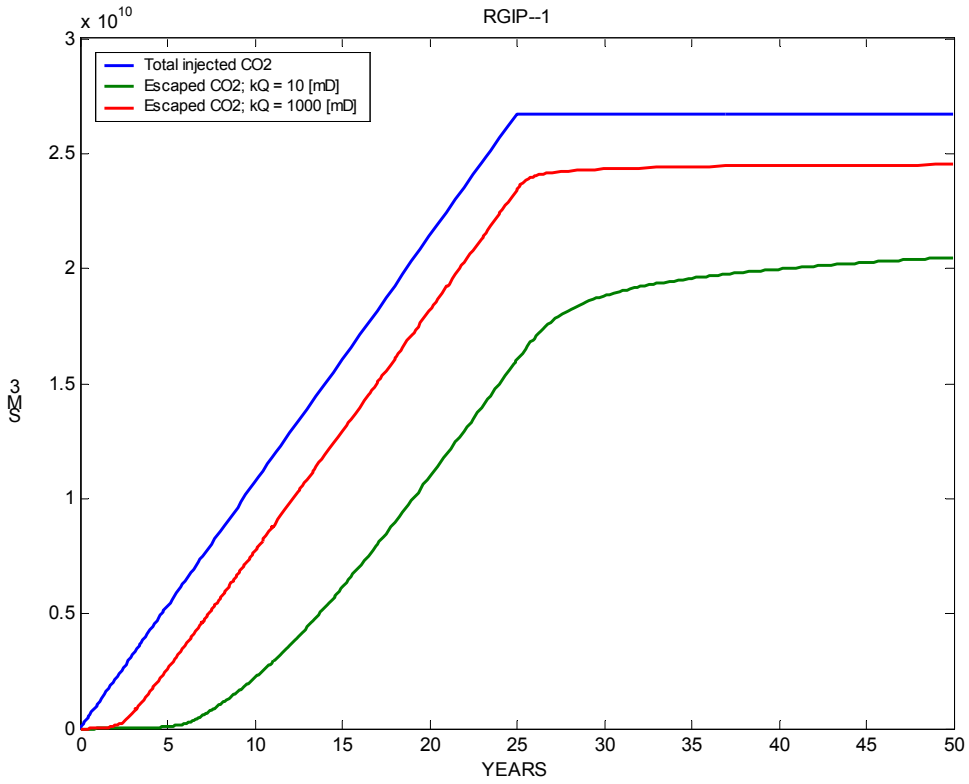

Figure 33 *Simulated cumulative volume of CO_2 leaked from the reservoir for the case of injection into the 'Garn' Formation only, for two high seal permeabilities (kQ).The cumulative injected volume of CO_2 is also shown.*

5. DISCUSSION AND CONCLUSIONS

The simulation results presented in the previous chapter show some general features:

- For a low-permeable seal, pressure build-up in the reservoir is too large to avoid hydraulic fracturing of the seal; fracturing of the seal, however, would dramatically increase its permeability leading to high leakage rates.
- For a high-permeable seal, leakage rates are very high, also in cases with strongly reduced reservoir permeability.

Some effects have not been included in the simulations that could improve the results somewhat. One effect is drainage (water outflow) into and through adjacent formations, such as the other sedimentary formations in the model or the basement. Outflow could reduce pressure build-up. However, outflow rates are expected to be small and will not significantly alter the overall results.

The capillary entry pressure for the seal was set to 0 in the simulations. This implies that CO_2 can enter the seal and flow through it as soon as it reaches it, irrespective of its capillary pressure. Accordingly the simulations overestimate the leakage rate. However, for the case of a high-permeable seal, capillary entry pressure would be low and the improvement of seal performance would thus be small.

Acceptable leakage rates for reservoirs are presently discussed in the scientific community. A major requirement for underground CO_2 storage sites would be that leakage from them into the atmosphere should not cause worse climatic conditions in the future than we can expect in the case of direct emission. Recent work indicates that the average storage time should be of the order of a few thousand years or more (Lindeberg 2002) or that annual leakage rates from each single storage site should be less than 0.01 % of the total injected CO_2 (Tore Torp, pers. comm 2004 on discussions in the IPCC work group on underground CO_2 storage, Hepple & Benson 2002).

The simulation results for the Beitstadfjord show that leakage rates from this site will probably be much higher than acceptable for the case of 25 years of injection with 2 million tonnes CO_2 injected per year. A rough estimate, scaling simulated pressure increases down by a factor of 20, is that also injection of only 5 % of the produced CO_2 from a power station (that is 100 000 tonnes CO_2 per year) will lead to too high pressures in the case of a low permeable seal. A reduced injection rate will reduce the absolute leakage rate in the high-permeable seal cases, but the relative leakage rate as a proportion of the total injected volume will most likely not be much reduced, because buoyancy as the the main driving force is still acting.

In conclusion, the Beitstadfjord Basin is not suitable for underground CO_2 storage, neither for storage at a high rate of 2 million tonnes per year nor at a lower rate of 100 000 tonnes per year.

The main disadvantage with the Beitstadfjord Basin as a storage site is the size of the availabe pore volume, which is much too small. Other critical properties are the lack of a trap and the low thickness and mechanically weak state of its Quaternary seal.

6. REFERENCES

Bjørlykke, K. 1999: Principal aspects of compaction and fluid flow in mudstones. In: Aplin, A.C., Fleet, A.J., & Macquaker, J.H.S. (eds.): Muds and Mudstones: Physical and Fluid Flow Properties. Geological Society, London, Spwecial Publications, 158, pp. 73-78.

Blikra, L.H., Mauring, E., Rønning, J.S. & Tønnesen, J.F. 1991: Geofysiske metoder ved kartlegging av løsmasser. Et eksempel fra Henning i Nord-Trøndelag. NGU Skrifter nr. 103, 1-20.

Blystad, P, Brekke, H., Færseth, R.B., Larsen, B.T., Skogseid, J. & Tørudbakken, B. 1995: Structural elements of the Norwegian continental margin. NPD-Bulletin No 8, 45 pp.

Bøe, R. & Bjerkli, K. 1989: Mesozoic sedimentary rock in Edøyfjorden and Beitstadfjorden, Central Norway: Implications for the structural history of the Møre-Trøndelag fault zone. Marine Geology 87, 287-299.

Bøe, R., Magnus, C., Osmundsen, P.T. & Rindstad, B.I. 2002: CO2 point sources and subsurface storage capacities for CO2 in aquifers in Norway. NGU Report 2002.010, 132 pp.

Ehrenberg, S.N. 1990: Relationship between diagenesis and reservoir quality in sandstones of the Garn Formation, Haltenbanken, mid-Norwegian continental shelf. Bulletin American Association of Petroleum Geologists 74, 1538-1558.

Gabrielsen, R.H., Odinsen, T., & Grunnaleite, I. 1999: Structuring of the northern Viking Graben and the Møre Basin; the influence of basement structural grain, and the particular role of the Møre-Trøndelag Fault Complex. Marine and Petroleum Geology 16, 443-465.

Hepple, R.P. & Benson, S.M. 2002: Implications of surface seepage on the effectiveness of geological storage of carbon dioxide as a climate change mitigation strategy. In: Gale, J. & Kaya, Y. (eds.): Greenhouse Gas Control Technologies (Proceedings of the 6th International Conference on Greenhouse Gas Control Technologies, Kyoto, Japan, october 2002), vol 1, pp. 261 – 266, Pergamon, Oxford (UK).

Koch, J.-O. & Heum, O.R. 1995: Exploration trends of the Halten Terrace. In: Hanslien, S. (ed), Petroleum Exploration and Exploitation in Norway, NPF Special Publication 4, 235-251.

Lindeberg, E. & Bergmo, P. 2003: The long-term fate of CO_2 injected into an aquifer. In: Gale, J. & Kaya, Y. (eds.): Greenhouse Gas Control Technologies (Proceedings of the 6th International Conference on Greenhouse Gas Control Technologies, Kyoto, Japan, october 2002), vol 1, pp. 489 – 494, Pergamon, Oxford (UK).

Lindeberg, E. 2003: The quality of a CO_2 repository: What is the sufficient retention time of CO_2 stored underground? In: Gale, J. & Kaya, Y. (eds.): Greenhouse Gas Control Technologies (Proceedings of the 6th International Conference on Greenhouse Gas Control Technologies, Kyoto, Japan, october 2002), vol 1, pp. 255 – 260, Pergamon, Oxford (UK).

Lindeberg, E., van der Meer, B., Moen, A., Wessel-Berg, D. & Ghaderi, A. 2000: Saline Aquifer CO_2 Storage (SACS): Task 2: Fluid and core properties and reservoir simulation. Report period: 01/11/98 – 31/12/99, SINTEF Petroleum Research, Report no. 54.5148.00/02/00

Mørk, M.B., Johnsen, S.O. & Torsæter, O. 2003: Porosity and permeability examination of Jurassic samples from Froøyane. Unpublished report, 5 pp.

Oftedahl, C. 1972: A sideritic ironstone of Jurassic age in Beitstadfjorden, Trøndelag. Norsk Geologisk Tidsskrift 52, 123-134.

Oftedahl, C. 1975: Middle Jurassic graben tectonics in Mid-Norway. Proceedings of the Jurassic northern North Sea Symposium, Stavanger. Norwegian Petroleum Society, Oslo, 1-13.

Riis, F. 1996: Quantification of Cenozoic vertical movements of Scandinavia by correlation of morpological surfaces with offshore data. Global and Planetary Change 12, 331-357.

Sheriff, R.E. 1989: Geophysical Methods. Prentice Hall, New Jersey, 605 p.

Sommaruga, A., & Bøe, R. 2003: Geometry and subcrop maps of shallow Jurassic basins along the Mid-Norway coast. Marine and Petroleum Geology 19, 1029-1042.

Twiss, R.J. & Moore, E.M. 1992: Structural geology. 532 pp., W.H., Freeman & Co, New York (US).

Weisz, G. 1992: An investigation of Jurassic coals from Haltenbanken and Beitstadsfjorden. A comparison of composition and maturity. Diploma thesis at the Department of Geology and Mineral Resources, Technical University of Trondheim (NTNU), Trondheim, Norway, 79 pp.